Review of micro modeling and regional modeling in geostatistics with focus on McMurray data

Mohammad Mahdi Badiozamani, Yashar Pourrahimian, Mohammad Tabesh
Mining Optimization Laboratory (MOL)
University of Alberta, Edmonton, Canada

Abstract

Predicting the performance of in-situ recovery processes is required to optimize development, planning and resource management in mining and petroleum projects. In this paper, two different concepts are presented; micro modeling and regional modeling.

In the first part of this paper, vertical permeability in the McMurray formation is estimated by micro modeling and a consistent numerical modeling framework based on core data, core photographs, high resolution image logs, and detailed geological interpretation. The framework includes dividing the stratigraphic column into facies with similar spatial arrangement of sand/shale, constructing high-resolution models of sand/shale, assigning porosity and permeability to sand/shale, calibrating the models to direct measurements, solving for effective horizontal and vertical permeability at the appropriate scale and transferring the results to geomodeling.

Multiple reservoir parameters should be mapped to assess the economic viability of a particular site. Some of these parameters considered in this research are structure, gross and net thickness, amount of contained bitumen. There are others which should be taken into account in more in-depth studies. In the second part of this paper, the reservoir of McMurray formation is characterized by 2D geostatistical modeling.

1. Introduction

The McMurray formation in the Athabasca oil sands deposits of Northern Alberta is part of the world's second largest proven crude oil reserves. The formation is characterized by stratigraphic layers that correspond to three different depositional environments: Marine, Estuarine and Fluvial facies. The McMurray Formation contains a vast resource of heavy oil. The economic production of this heavy oil often makes use of thermal processes to reduce viscosity and horizontal wells that have a large contact area with the formation. Steam is often injected to introduce thermal energy. The rates of steam rise and water/oil drainage are predicted by flow simulation. A critical input parameter in that flow simulation is the vertical permeability. Accurate prediction of fluid flow would permit optimization of the recovery process and operating parameters; thus, accurate estimation of vertical permeability is of great interest in the McMurray formation.

The sands in the McMurray formation are host to the crude bitumen, in which three main lithofacies are recognized based on the depositional environments: Fluvial, Estuarine and Marine from the base to the top of the formation. Stratigraphic subdivisions for the McMurray formation include the lower, middle and upper McMurray. There are a lot of studies and historical overviews about the McMurray. Total remaining established reserves of crude bitumen in Alberta are estimated at more than 27 billion cubic meters, or imperial equivalent in excess of 175 billion barrels. This includes about 22.6 billion m^3 of in-situ bitumen, of which 0.5 billion m^3 are from

lands under active development. Surface-mineable crude bitumen reserves amount to 5.2 billion m^3 , of which 1.4 billion m^3 are from lands under active development (Hein & Cotterill, 2000).

The major bitumen reserves of Alberta are hosted within four major oil sands deposits in northern Alberta, the Athabasca, Wabasca, Cold Lake, and Peace River deposits. Some of recent studies have recommended that the informal term 'Middle McMurray' be abandoned, and what was formerly, mapped as Middle McMurray now be included as part of the Upper McMurray. What was formerly designated as 'basal' or 'lower' McMurray is called Lower McMurray. In summary, it is proposed that the two mappable informal members of the McMurray formation are the Lower McMurray and Upper McMurray, which are separated by a disconformity (Hein & Cotterill, 2000).

The ability of the reservoir formation to transmit fluids (permeability) has a large effect on the reservoir response for given operating conditions. Permeability is a constant value that relates the flow rate through a porous medium to an imposed pressure gradient. Small-scale variations in the clastic deposits of the McMurray cause permeability to be variable and direction dependent. Permeability in the vertical direction is of primary concern because operators are concerned with (1) the rise of steam through the formation, (2) the possible escape of steam and thermal energy to overlying formations, and (3) the rates at which condensed water and oil will drain to horizontal production wells (C. V. Deutsch, 2009).

The micro modeling part of this paper is concerned with absolute vertical permeability. There are important confounding effects that are not considered such as changes to permeability because of multiple fluids present in the formation and changes to permeability because of time varying geomechanical effects. This paper is primarily concerned with the influence of small scale geological heterogeneities on the estimation of vertical permeability.

Multiple reservoir parameters should be mapped to assess the economic viability of a particular site. These parameters include but are not limited to structure, gross and net thickness, amount of contained bitumen, the presence of shale and the presence of water and gas zones. In most cases, these geological variables are 2D summaries for particular productive horizons. A complete study may require the mapping of 20 to 30 variables. Hydrocarbon resources are calculated as a combination of these variables. If 2D models have a good quantitative measure of reservoir parameters, we can estimate resources without building 3D models. In addition, 2D modeling is simpler and faster than 3D modeling, and especially useful in modeling a large area where the complex 3D geostatistical models may not be practical. The regional modeling part of this paper demonstrates the reservoir characterization of the McMurray formation by 2D geostatistical modeling (Ren, Mclennan, Leuangthong, & Deutsch, 2006).

2. Installing required software

In order to do the Geostatistical modeling some software is required. It was decided to use a set of free Geostatistical tools as well as general software as mentioned in Table 1.

3. Micro modeling

For micro modeling, four steps should be done. These steps are as follows (1) process the image to create a scaled sand-shale indicator image with known spatial coordinates, (2) assign 3D sand-shale indicator, porosity and permeability values, (3) solve for the effective horizontal and vertical permeability, and (4) summarize and check the results for subsequent mini modeling.

Table 1. Required software

#	Software Name	Description	Website
1	Notepad ++	A professional open source text editor	http://Notepad-plus.sourceforge.net
2	GSView	A postscript file viewer	http://pages.cs.wisc.edu/~ghost/gsview/
3	FSViewer	An open source image viewer/editor	http://www.faststone.org/FSViewerDownload.htm
4	Cygwin	A command prompt application based on Linux syntax	http://www.cygwin.com
5	SGeMS	A free set of Geostatistical tools provided by Stanford university	http://sgems.sourceforge.net
6	GSLib	A free command based set of Geostatistical tools by Clayton Deutsch and Manu Schnetzler.	http://gslib.com
7	MS Excel	A commercial spreadsheet used for doing some statistical operations and charting	http://office.microsoft.com

3.1. Facies Modeling

In the beginning, core photographs or image logs were provided. The image must be cropped and saved as a gray scale image for processing. The scale of the image must be recorded for processing. Then, the continuous gray scale value must be converted to sand-shale indicator values (C. V. Deutsch, 2009). In this case, we have categorical variables. There are only sand and shale. The indicator variables are defined by:

$$i(u_\alpha, \mathrm{s}) = \begin{cases} 1, & \text{if sand is present at location } u_\alpha \\ 0, & \text{otherwise} \end{cases} \quad (1)$$

We have usually a set of data provided by labs or machines gathering data on the site. No matter whether the data is provided by machines or people, you have to clean some invalid records and outliers and select subsets of data for different purposes. The data provided for this project is the result of an image processing performed on the FMI data of a drill hole. The image is processed and resulted in a set of zero and ones regarding sand and shale. A set of points, which form a cylinder of 0.1m in height by 0.12m in radius, is selected for further modeling. The x and y coordinates of points are then calculated and the data required for creating the model is prepared by Clayton himself.

After gaining sand-shale indicator values for different slices, they are converted to GSLIB format and coordinates of each point with related indicator value is assigned. The sand-shale indicator data represents an annular volume. Fig. 1 shows part of preliminary data.

Fig. 2 shows part of data in GSLIB format. The columns of this figure indicate x, y, z, and facies, respectively. The annular volume has been made from 50 slices with 2 mm thickness, thus height of the cylinder is equal to 100 mm. For data visualization, Stanford Geostatistical Modeling Software (SGeMS) is used, which is a well-prepared package to visualize and manipulate the

geostatistical data. Two views of FMI data are shown in Fig. 3. Red areas and blue areas indicate sand and shale, respectively. Plan view and location of FMI data are shown in Fig. 4.

In order to have a better understanding of the data, some basic statistical operations has been done in MS Excel. The file has been imported into Excel as a space-delimited file. The zero-one values regarding sand/shale are average using subtotals in each vertical level and globally. The results can be found in Table 2. A global average of 0.6491 and a standard deviation of 0.4772 are the results of the calculation. By adding two trend lines to the chart, it can be inferred that there is an obvious downward trend in the proportion of sand in each level. As the value for z (which stands for elevation) goes up the average amount of sand goes higher with almost less standard deviation. Another trend study that seems to be useful is to do the averaging over different sectors of the cylinder. The cylinder was divided into four area based on coordinates axes. Fig. 5 shows specifications of each region. The percentages of sand and shale within each area are shown in Fig. 6. The most outstanding feature of Fig. 6 is the percentage of sand within area 1. It can be seen that only in the third area, percentage of shale is a little more than sand.

3.2. Calculate and model variograms

The variogram is function of distance and direction. Variogram inference proceeds in three main steps (Leuangthong, Khan, & Deutsch, 2008):

1. Calculate the experimental variogram in multiple directions for a number of lags that approximately correspond to the average spacing between data,
2. Interpret the experimental variogram points and supplement them with expert judgment or analogue data,
3. Fit a valid parametric model to the directional variograms in all directions.

The variogram is needed for distance up to 1m. The vertical variogram is well defined from the well logs. According to the given data, the horizontal variogram should look the same as the vertical one but with a range five times larger than the vertical one.

To calculate the vertical variogram, the normal scores of porosity within sandy IHS facies should be used; therefore, the porosity values for facies 2 are transferred to normal unit.

The variogram is usually measured in two horizontal and one vertical direction. The data we have is distributed over the lateral surface of a cylinder. Thus, calculating vertical variogram would be an ordinary job. The variogram is calculated using the "gamv" application available in GSLib (C.V. Deutsch & Journel, 1998) and the parameter file presented in Table 3.
The dip tolerance and lag tolerance values have been assumed to be small values to make sure each point is paired with only one other point. Since there is enough data and it is regularly spaced, the assumption seems to be reasonable. We usually want to have variograms for lags smaller that ¾ of the total length of the domain. Consequently, the number of lags and lag separation distance are considered 40 and 0.002, respectively ($40 * 0.002 = 0.08 \cong \frac{3}{4} * 0.1$).

```
 RADIUS 0.59999999E-01
NSLICE    1000
STHICK 0.30000000E-02
NANG       365
11111111111111100000000000000000000000000110000000000000000000000000000000000
11111111111111110000000000000000000010000110000000000000000000000000000000000
11111111111111110000000000000000000111111111000000000000000000000000000000000
11111111111111110000000000000000000111111111000000000000000000000000000000000
11111111111111110000000000000000000111111000000000000000000000000000000000000
```

Fig. 1. Sand-shale indicator values

```
FMI Data for 615
4
X
Y
Z
Facies
.0600 .1200 .0010 1
.0610 .1200 .0010 1
.0621 .1200 .0010 1
.0631 .1199 .0010 1
```

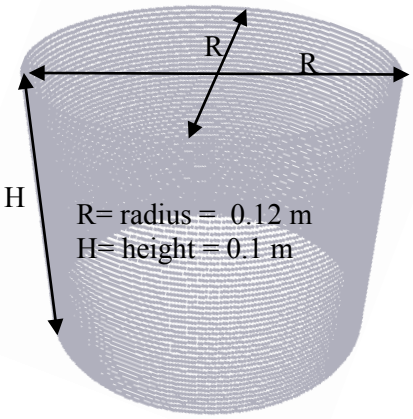

Fig. 2. Part of the created FMI.dat file and related coordinates

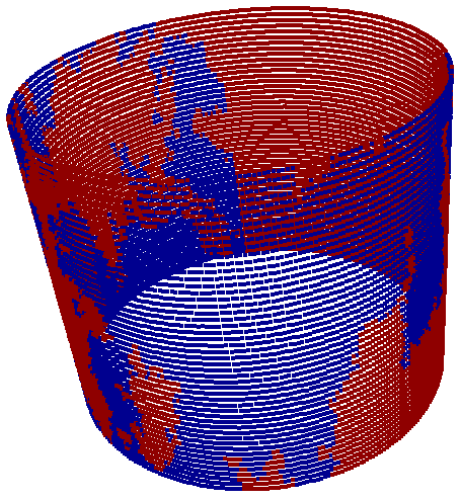

Fig. 3. 3D view of FMI data

Table 2. Level Based Averages

Z	Facies (Average)	Facies (StdDev)
0.099	0.5781	0.4945
0.097	0.6137	0.4876
0.095	0.6411	0.4803
0.093	0.6411	0.4803
0.091	0.6192	0.4863
0.089	0.6027	0.4900
0.087	0.5890	0.4927
0.085	0.5616	0.4969
0.083	0.5699	0.4958
0.081	0.5781	0.4945
0.079	0.5616	0.4969
0.077	0.5671	0.4962
0.075	0.5562	0.4975
0.073	0.5671	0.4962
0.071	0.5671	0.4962
0.069	0.5918	0.4922
0.067	0.6000	0.4906
0.065	0.6000	0.4906
0.063	0.6384	0.4811
0.061	0.6795	0.4673
0.059	0.6740	0.4694
0.057	0.6685	0.4714
0.055	0.6630	0.4733
0.053	0.6548	0.4761
0.051	0.6521	0.4770
0.049	0.6822	0.4663
0.047	0.6575	0.4752
0.045	0.6411	0.4803
0.043	0.6740	0.4694
0.041	0.6740	0.4694
0.039	0.6822	0.4663
0.037	0.6685	0.4714
0.035	0.6795	0.4673
0.033	0.7096	0.4546
0.031	0.7205	0.4493
0.029	0.7233	0.4480
0.027	0.7315	0.4438
0.025	0.7233	0.4480
0.023	0.7068	0.4558
0.021	0.7041	0.4571
0.019	0.7096	0.4546
0.017	0.7315	0.4438
0.015	0.7068	0.4558
0.013	0.7233	0.4480
0.011	0.7589	0.4283
0.009	0.7205	0.4493
0.007	0.6548	0.4761
0.005	0.6438	0.4795
0.003	0.6164	0.4869
0.001	0.5781	0.4945

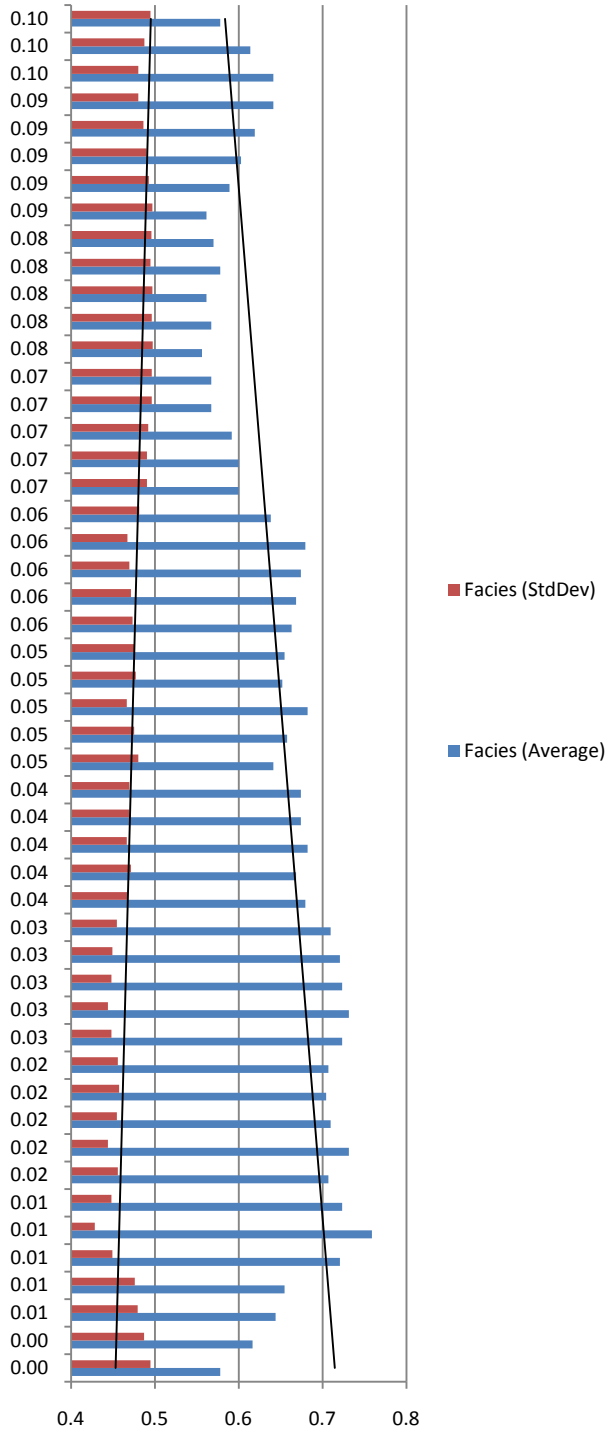

Fig. 4. Vertical trends

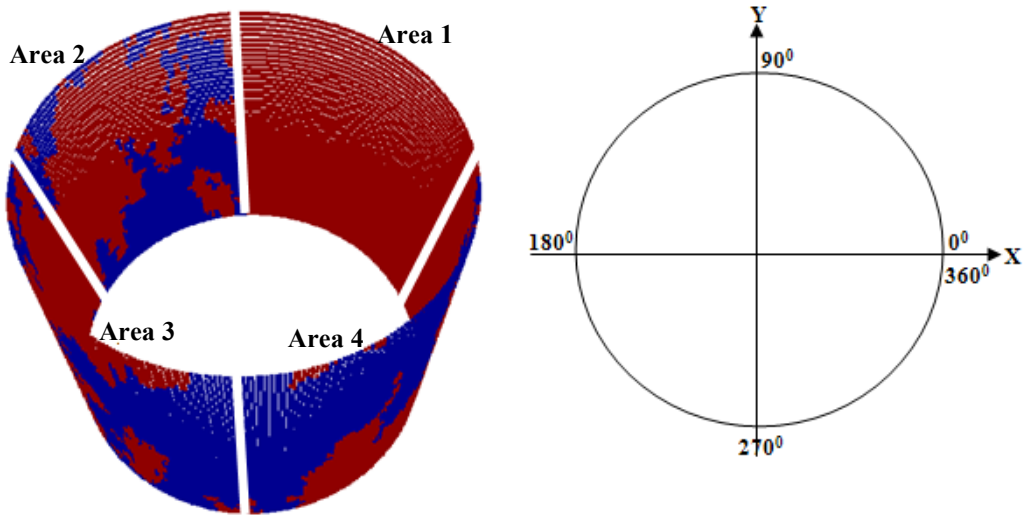

Area	Angle (β^0)	Coordinates
1	$0 \leq \beta \leq 90$	$0.06 \leq X \leq 0.12$, $0.06 \leq Y \leq 0.12$, $0.00 \leq Z \leq 0.1$
2	$90 \leq \beta \leq 180$	$0.00 \leq X \leq 0.06$, $0.06 \leq Y \leq 0.12$, $0.00 \leq Z \leq 0.1$
3	$180 \leq \beta \leq 270$	$0.00 \leq X \leq 0.06$, $0.00 \leq Y \leq 0.06$, $0.00 \leq Z \leq 0.1$
4	$270 \leq \beta \leq 360$	$0.06 \leq X \leq 0.12$, $0.00 \leq Y \leq 0.06$, $0.00 \leq Z \leq 0.1$

Fig. 5. Specified areas to determine the proportion of sand to shale

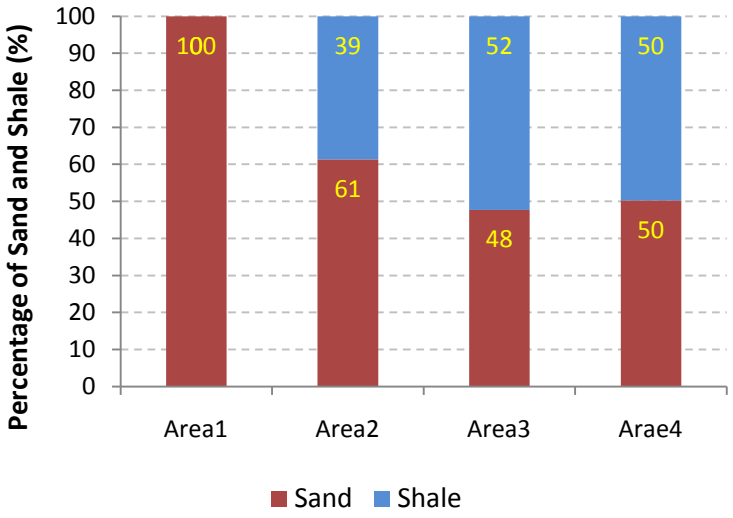

Fig. 6. Percentage of sand and shale within each area

Table 3. Parameter file used for calculating vertical variogram

Parameters for GAMV START OF PARAMETERS:	
fmi.dat	-file with data
1 2 3	-columns for X, Y, Z coordinates
1 4	-number of variables, col numbers
-1.0e21 1.0e21	-trimming limits
vgamv.out	-file for variogram output
40	-number of lags
0.002	-lag separation distance
0.0005	-lag tolerance
1	-number of directions
0.0 90.0 50.0 -90.0 0.1 50.0	-azm,atol,bandh,dip,dtol,bandv
0	-standardize sills? (0=no, 1=yes)

On the other hand, when horizontal variogram is going to be calculated, there would not be enough data to judge the maximum and minimum direction of continuity based on the available data. Therefore, an omni-directional horizontal variogram is used. The maximum distance between pairs of data in horizontal direction is 0.12 meters. Thus, we can consider 40 lags with a distance of 0.0025 ($40 * 0.0025 = 0.1 \cong \frac{3}{4} * 0.12$). Since the points are not distributed regularly, we have considered a larger lag tolerance to make sure there will be enough pairs of data to calculate the variogram. Since the FMI data points are aligned in the surface of a completely vertical cylinder, the azimuth angle for both directions is set to zero, with the azimuth tolerance equal to 90 degrees that covers the whole vertical cylinder surface. The direction of vertical cylinder also implies to set the dip angle to -90 degrees for vertical and 0 degree for horizontal directions. Because the data points are regularly spaced, a small dip tolerance, 0.1 degree, is suitable for variogram calculation.

The two experimental variograms can be found in Fig. 7. Red bullets stand for experimental vertical variogram whereas blue ones represent the experimental horizontal variogram.

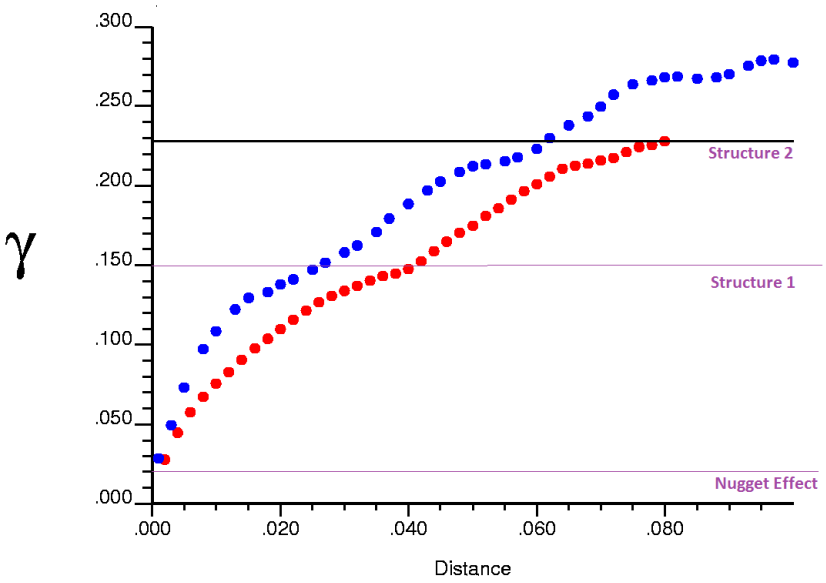

Fig. 7. Experimental variogram

Looking at variograms in two directions, using two or three nested structures seems to be reasonable. In this case, three variance regions can be defined for three horizontal and vertical variograms, the first one is a nugget effect, and the second one is exponential variogram structure. The last one is spherical variogram structure. The variogram parameters corresponding to the variogram shown in Fig. 8 have been summarized in Table 4.

$$\gamma(h) = 0.02 + 0.13\, Exp_{\substack{a_{h\max}=0.08 \\ a_{h\min}=0.08 \\ a_{vert}=0.026}}(h) + 0.078\, Sph_{\substack{a_{h\max}=0.1 \\ a_{h\min}=0.1 \\ a_{vert}=0.06}}(h) \tag{2}$$

Table 4. Variogram model corresponding to variogram shown on Fig. 8

Variance Contribution	Type of Variogram	Horizontal Range, m	Vertical Range, m
0.02	Nugget		
0.13	Exponential	0.08	0.026
0.078	Spherical	0.1	0.06

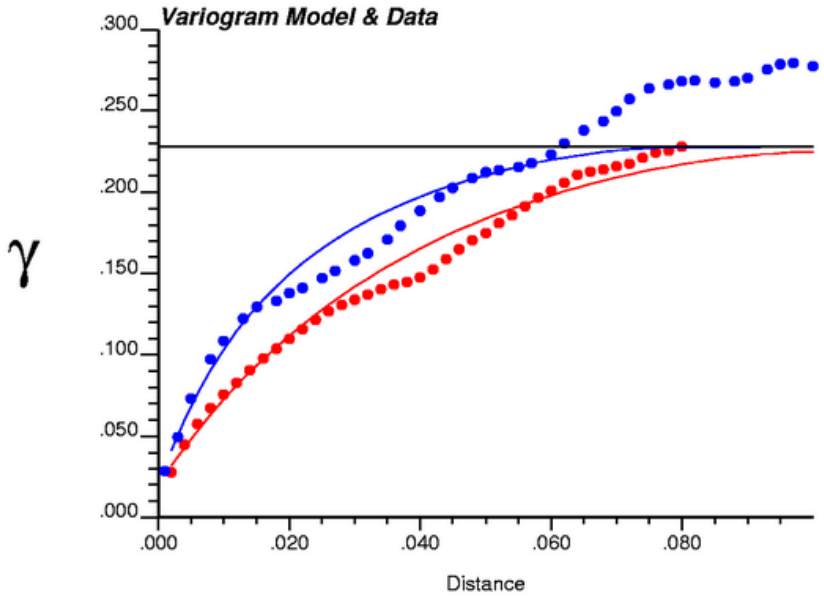

Fig. 8. Variogram models

3.3. Kriging

Kriging is the most important one among traditional mapping applications and an essential component of geostatistical simulation methods. In this section, we want to construct a model of spatial uncertainty characterizing the distribution and occurrence of the facies. There are 18250 records of data that should be used to estimate unsampled locations inside the domain. Fig. 9 shows

the domain and sampled locations. In this case, Simple Kriging (SK) is done using the variogram model provided in Eq. (2). For Kriging 50×50×50 grid nodes is used. Size of each cell in X, Y and Z directions are 2.4 mm, 2.4 mm, and 1.0 mm respectively. Fig. 9 schematically shows how the initial cylinder shape surface, containing well log data, is transferred to a cube through Kriging. In order to perform SK estimation, a search ellipsoid is defined with maximum search radius of 90 mm in all three directions and zero angles. 25 to 35 points are used to estimate the facies of each grid cell.

The result of the 3D SK operation is illustrated in 3D in Fig. 10. Three orthogonal planes in the middle of the domain are also presented in Fig. 11. Kriging has been implemented using the "kt3d.exe" application in GSLib. Simple Kriging method uses available values at sampled locations as well as variogram models to predict values at unsampled locations. In order to check if the Kriging procedure is on track, cross validation seems to be useful. In cross validation, values at some sampled locations are assumed to be unknown and are predicted using the Kriging equations. Afterwards, the difference between actual and predicted values is plotted as shown in Fig. 12. A correlation value of 0.938 shows a reasonable estimate.

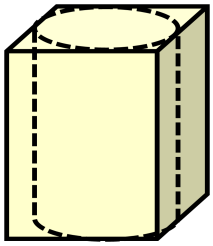

Fig. 9. Cylinder to cube transfer

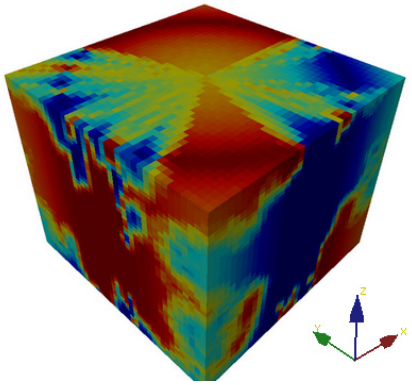

Fig. 10. Kriging 3D illustration

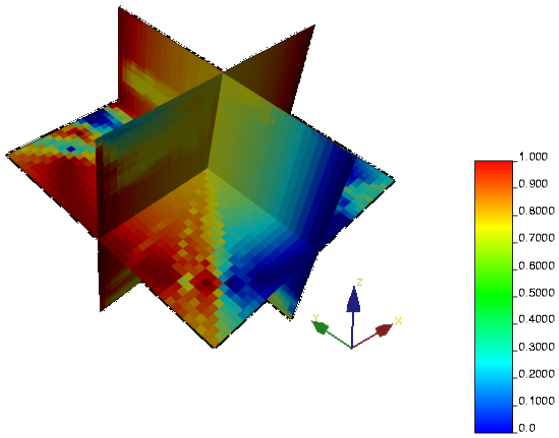

Fig. 11. Kriging planes

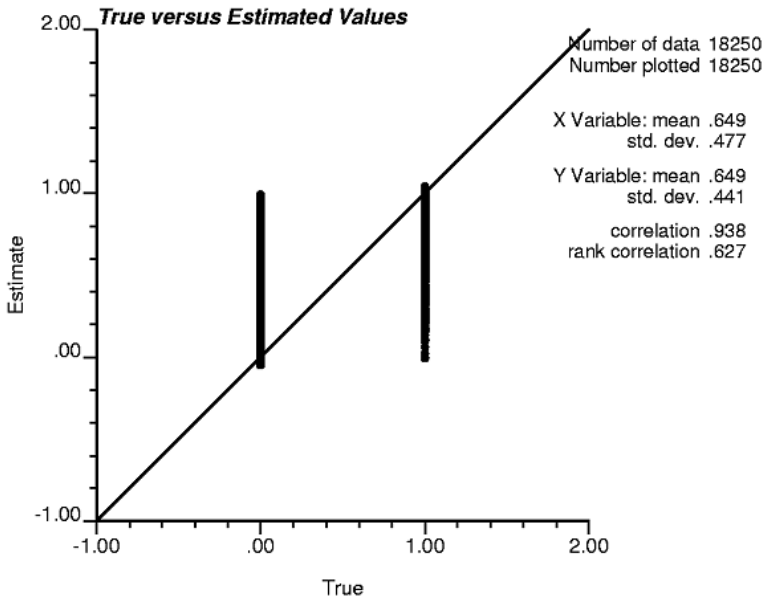

Fig. 12**.** True versus Kriged values

3.4. Simulation

3.4.1 Facies simulation

The next step is to simulate the facies in the grid. There is a drawback in Kriging which is called the smoothing effect. On the other hand, the illustrations in Fig. 3 and Fig. 4 are colored from blue to red which represent values between 0 and 1. We know that a special cell of the grid can only be zero or one (sand or shale) but these values indicate the chance of being 1 for each cell. In order to create realizations of facies values in each cell and also to overcome the smoothing effect of Kriging, simulation comes into mind.

Since the variable is a categorical variable, Gaussian simulation does not seem to be appropriate. Hence, Sequential Indicator Simulation is implemented using an application called "BlockSIS.exe". One hundred realizations are generated using this application. The first realization is illustrated in Fig. 13 and Fig. 14. Red points stand for sand whereas blue ones represent shale.

After generating 100 realizations it seems appropriate to compare the average result of the simulation with Kriging results. There is an application in GSLib which is responsible for averaging different realizations. This program which can calculate different statistics for different number of realizations is called "PostSim.exe" (see Fig. 15). In Fig. 16, some slices of Kriging and simulation are compared with each other. As it can be seen, the Kriging results are smoother than the simulation results. That is mainly because of smoothing effect of Kriging. However, by comparing the results of simulation and Kriging, it can be deduced that they are following the same pattern. In order to compare the closeness of simulation and Kriging results statistically, a scatter plot of post-simulation results and Kriging results is shown in Fig. 16. The correlation coefficient of the scattered data is 0.93. It can be inferred that the average of simulations converges to the Kriged estimates with an acceptable correlation coefficient.

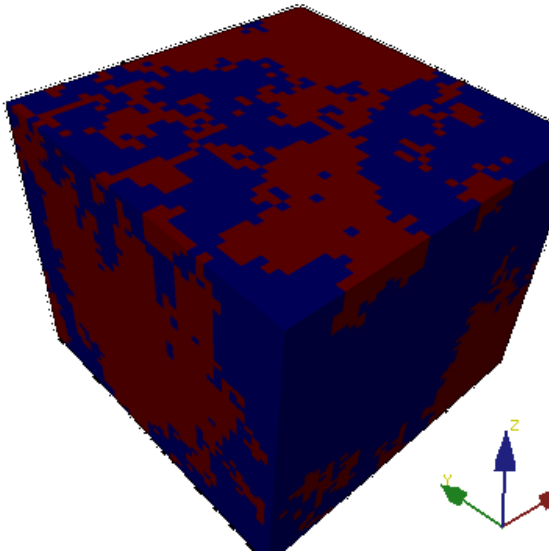

Fig. 13. Simulation result (3D)

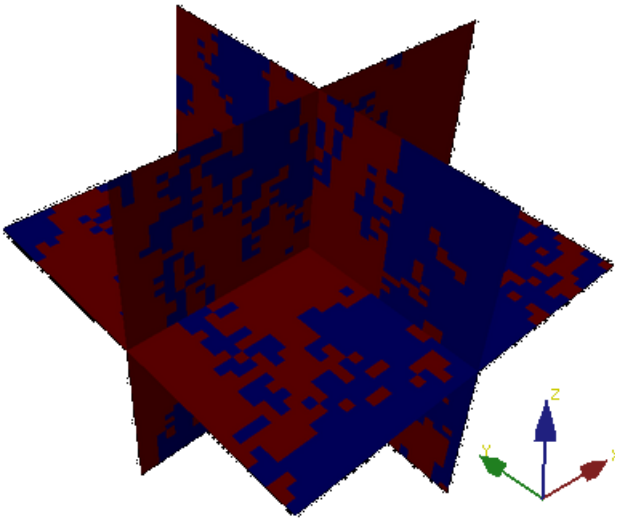

Fig. 14. Simulation result (Planes)

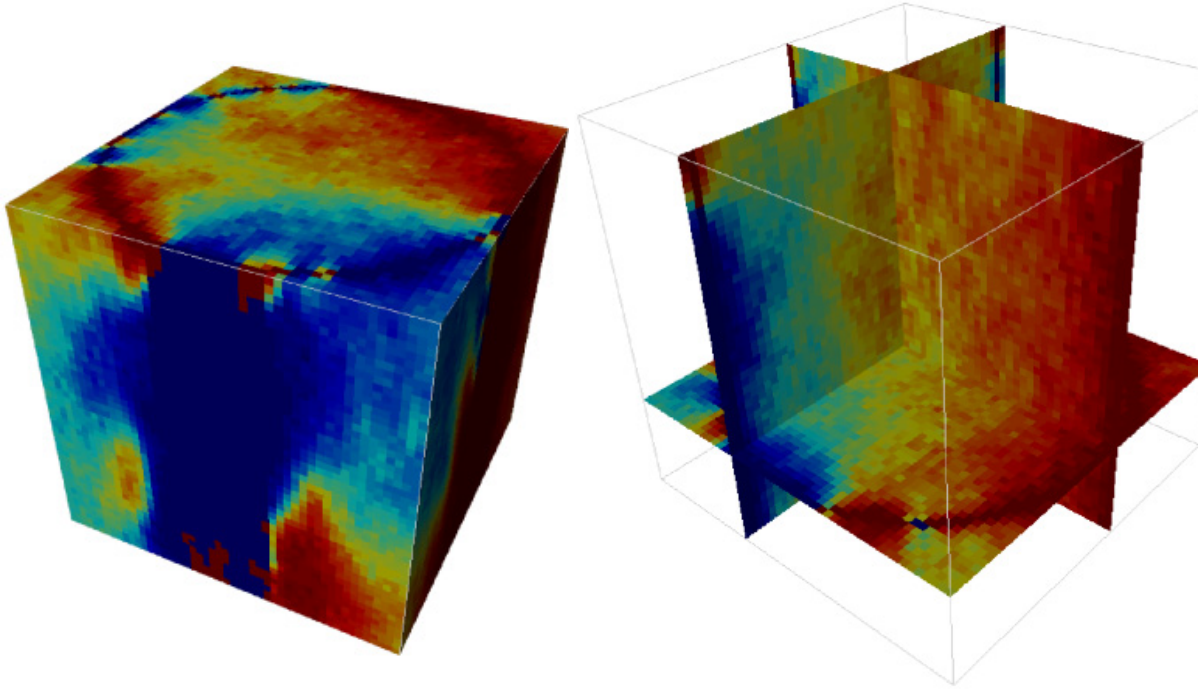

Fig. 15. 3D views of average of 100 realizations for facies (output of PostSim)

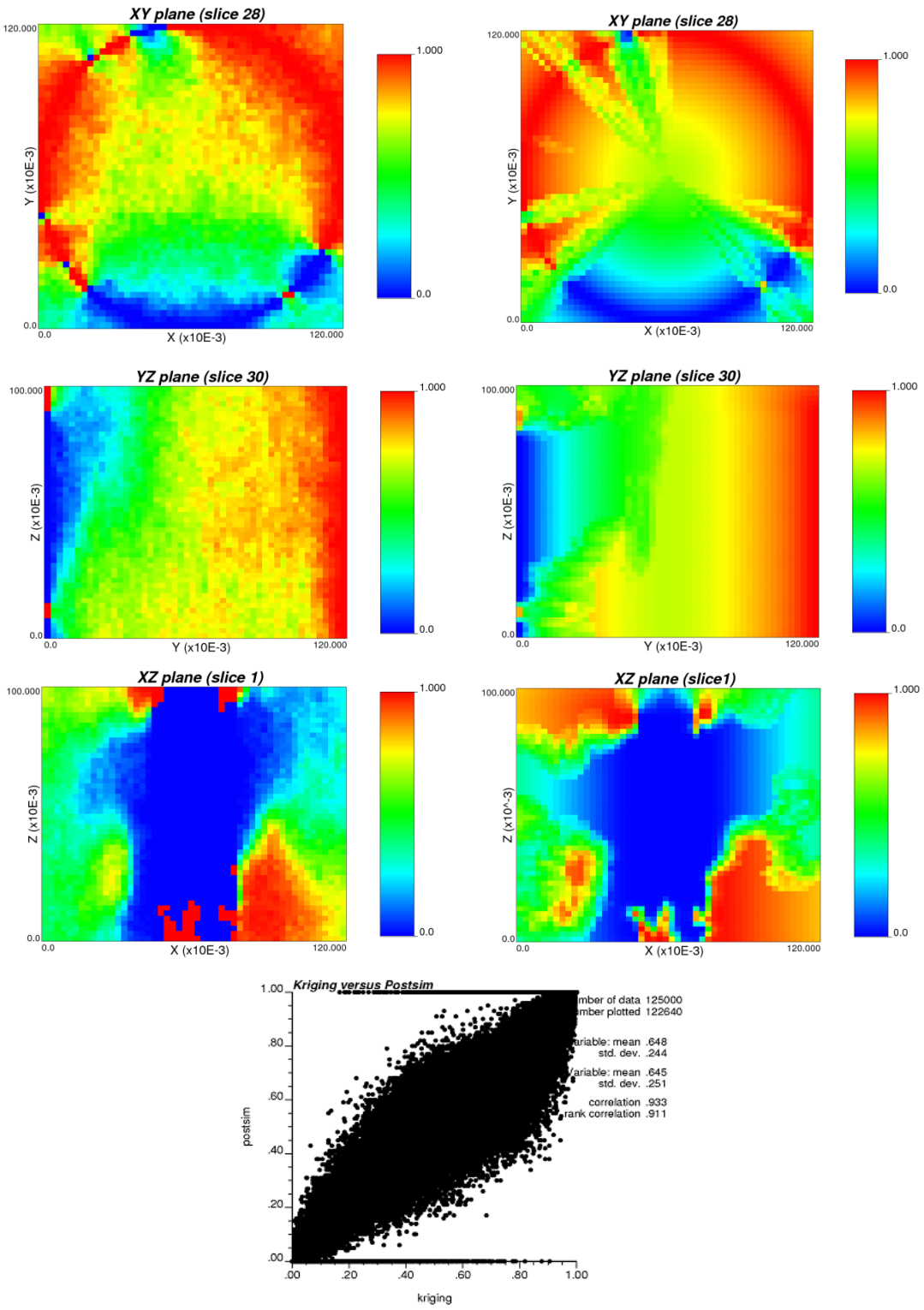

Fig. 16. Comparison between results of simple kriging and simulation of facies

3.4.2 Porosity and Permeability Simulation

In order to simulate the porosity and permeability, random Gaussian numbers are generated. The generated numbers then are transformed to the desired distribution. Permeability values are meant to have lognormal distribution with a mean and standard deviation of 4000 mD and 500 mD and 1 mD and 5 mD for sand and shale respectively. The parameters used to generate one hundred realizations for porosity and permeability are presented in Table 5.

The results of Normal generated numbers for porosity and permeability simulation are averaged two times, once before transferring to desired distribution and once after, to enable us to compare the statistics of generated data values with what it is supposed to be (Normal distribution with mean of 0 and variance of 1). The results are presented in Table 6.

The deviation of generated data from Normal (0, 1) is mainly because of the range of variogram considered in simulations. It is assumed that both porosity and permeability have the same isotropic spherical variogram with the range of 100 mm. Maybe with decreasing the range of variogram, using an anisotropic variogram or changing its type, the results could get closer to the Normal (0, 1).

The simulation results of porosity are used in permeability simulation. In other words, the permeability is simulated conditioned to the porosity, using collocated CoKriging. Correlation coefficient of 0.75 is used for collocated CoKriging. The results of simulated porosity and permeability are presented in Table 7. Fig. 17 shows the average histogram of one hundred realizations for porosity and permeability of sand and shale (Relating to Table 7). In addition to the histograms, it seems useful to check if the correlation between porosity and permeability values is respected. The scatter plot of the two sets of data is shown in Fig**.** 18.

Table 5. Parameters for porosity and permeability simulation

	distribution	particles	mean	STDev
Porosity	Normal	Sand	0.33	0.015
		Shale	0.01	0.005
Permeability(mD)	Log Normal	Sand	4000	500
		shale	1.0	5.0

Table 6. Statistics of generated data values for N (0, 1)

	distribution	particles	Mean	Std
Porosity	Normal	Sand	0.01	0.077
		Shale	0.05	0.094
Permeability(mD)	Normal	Sand	0.00	0.086
		shale	0.01	0.110

Table 7. Statistics of porosity and permeability simulation

	distribution	particles	mean	STDev
Porosity	Normal	Sand	0.33	0.001
		Shale	0.01	0.0005
Permeability(mD)	Log Normal	Sand	3999.39	43.41
		shale	0.958	0.335

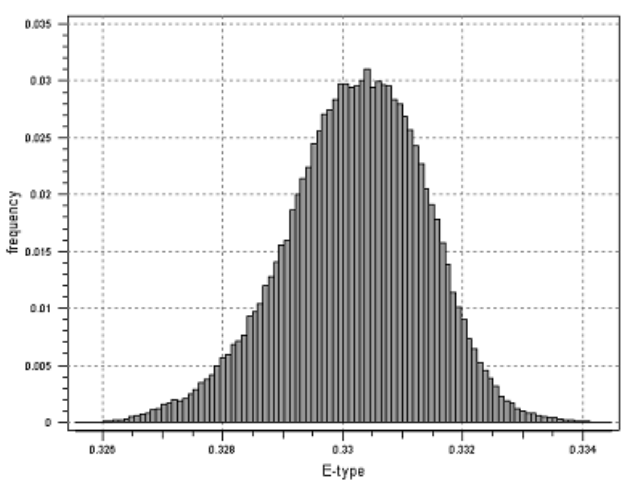

Simulation of sand porosity

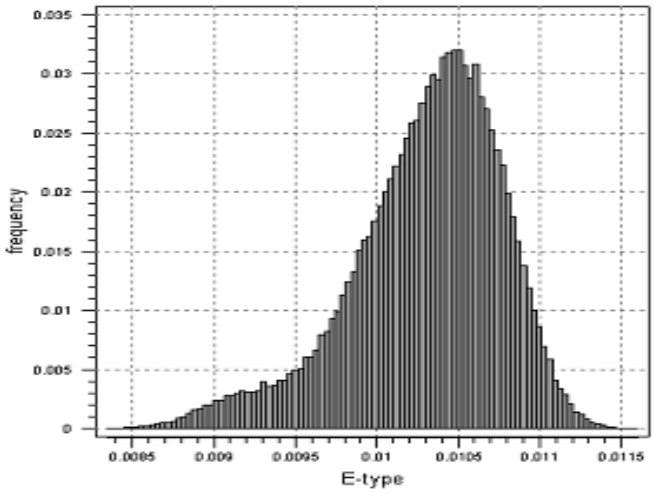

Simulation of shale porosity

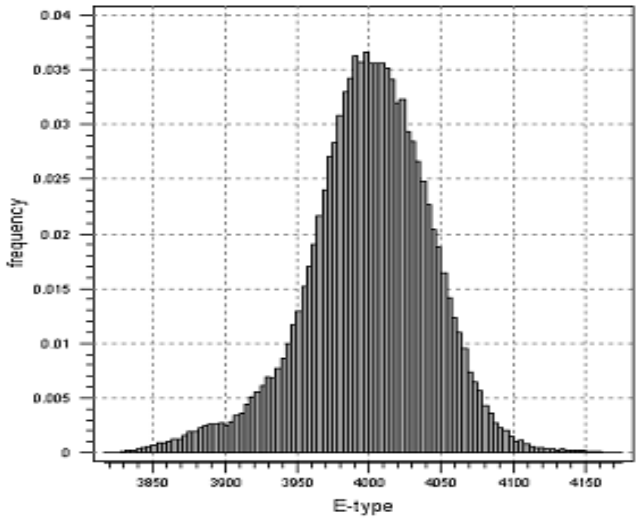

Simulation of sand permeability

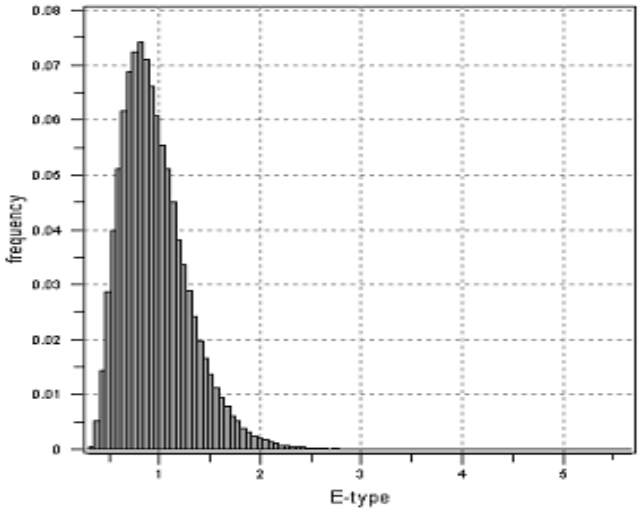

Simulation of shale permeability

Fig. 17**.** Histogram of 100 realizations for porosity and permeability of sand and shale

3.4.3 Merge porosity and permeability realizations with facies data

The domain we tend to study consists of two different facies. The first set of points is sand and the second ones are considered as shale. Each group has its own porosity and permeability values. But the final model of study consists of both groups and these values are needed to be merged before finding the porosity and permeability values for the whole block. To do so, “mergemod.exe” can help. In this application, sets of data are merged together based on different categories from another file. The categories are 0 and 1 in our case where 0 stands for shale and 1 for sand.

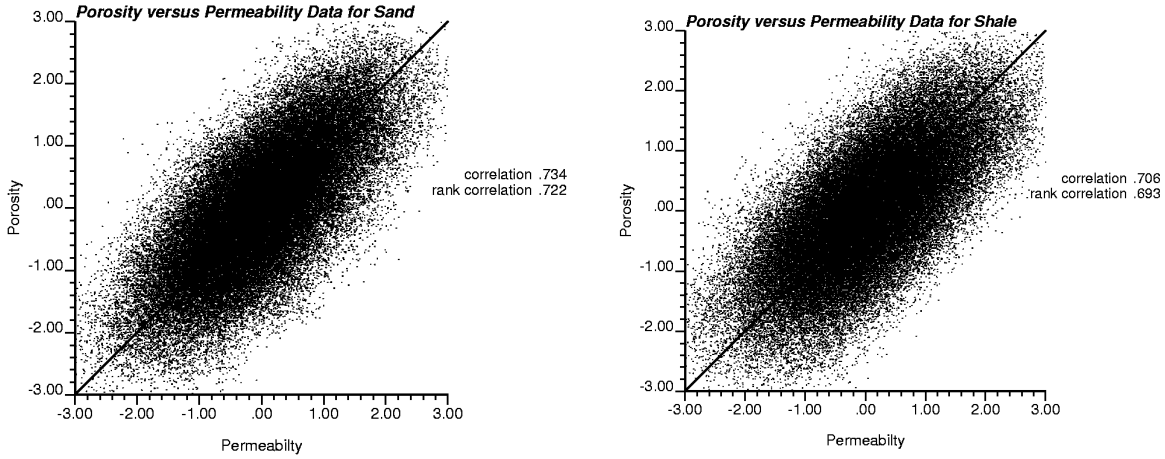

Fig. 18. Porosity versus permeability

Therefore, 100 realizations of porosity values for sand and 100 realizations of porosity values for shale are merged using 100 facies realizations. The same approach is taken for permeability values. Afterwards, the resulting datasets are averaged using "PostSim.exe" to have a better understanding of the results.

Output of BlockSIS (facies model)
Model of sand porosity (N(0.33,0.015)) } Must be merged
Model of shale porosity (N(0.01, 0.005))

Output of BlockSIS (facies model)
Model of sand permeability (lognormal(4000,500)) } Must be merged
Model of shale permeability (lognormal(1,5))

Average values for merged porosity and permeability are shown in Fig**.** 19. It can be seen that ups and downs of permeability and porosity values are correlated as expected. In addition, colors show significant similarity to average facies values. That happens because of the large difference between average porosity and permeability values for sand and shale. Wherever sand exists, higher porosity and permeability values are expected and vice versa.

3.4.4 Flow Simulation and effective permeability calculation

In order to find the porosity and permeability for the whole domain, the flow is simulated. The merged porosity and permeability are used in flow simulation. For this purpose "flowsim.exe" program is used. In the output file three directional permeability values, K_x, K_y and K_z is reported. In addition, the arithmetic, geometric and harmonic averages are also reported in output file. Histogram of effective horizontal and vertical permeabilities and arithmetic average of porosity are shown in Fig**.** 20. Table 8 represents summary of permeability results in the three principal directions. The arithmetic average of porosity is 0.215 with standard deviation of 0.016. According to the obtained results, permeability in vertical direction is higher than horizontal.

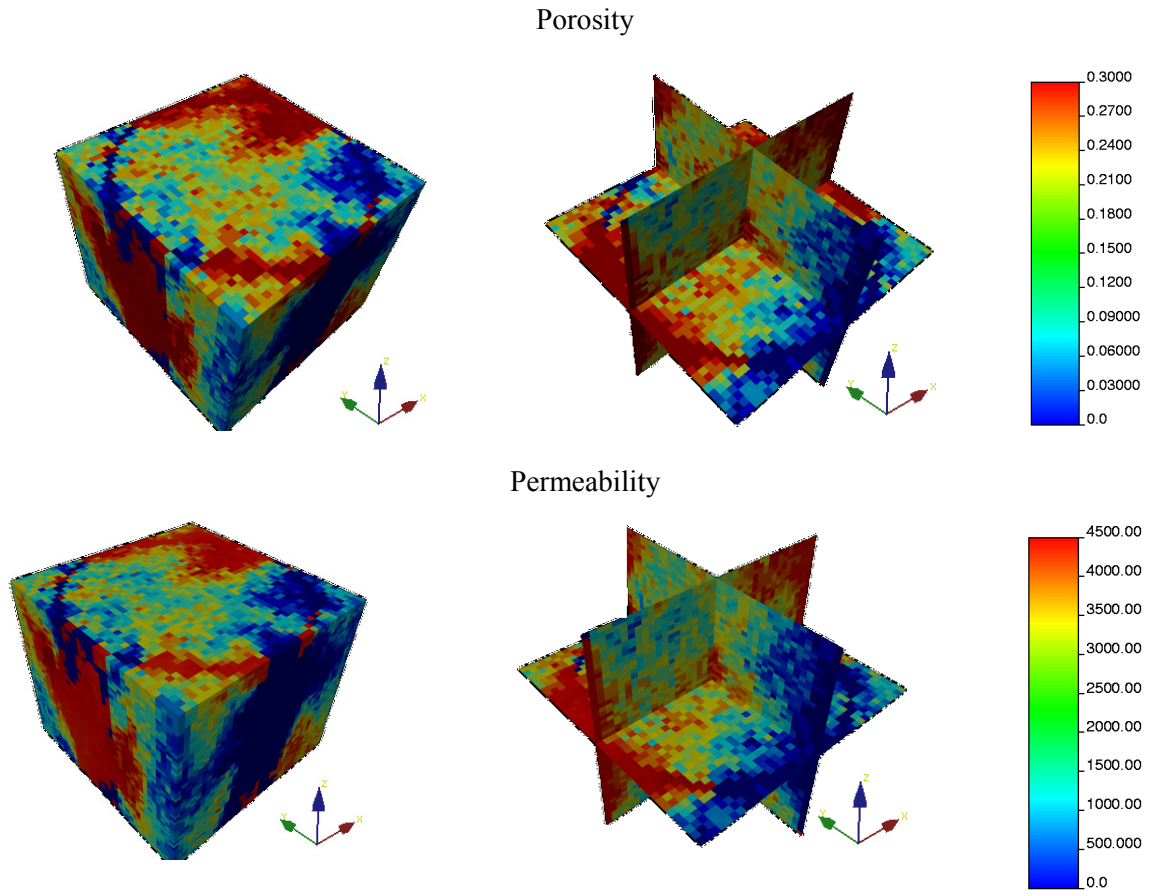

Fig. 19. Average values for merged porosity and permeability

Table 8. Results of permeability in x, y and z directions

Direction	**K_X**	**K_Y**	**K_H**	**K_Z**
Mean	1244.70	1058.28	1137.75	1885.37
Std.	383.60	180.047	249.80	258.33
Min.	377.415	589.99	527.78	13.11.46
Max	1973.68	1534.87	1645.18	2377.65

The relationship between K_H and ϕ, and the K_V/K_H ratio and K_H are the important results of the micro modeling because of their application in reservoir modeling at a large scale. These relationships are shown in Fig. 21. Correlation between K_V/K_H ratio and K_H is -0.85, that means increasing the K_V/K_H ratio, permeability in horizontal direction is reduced.

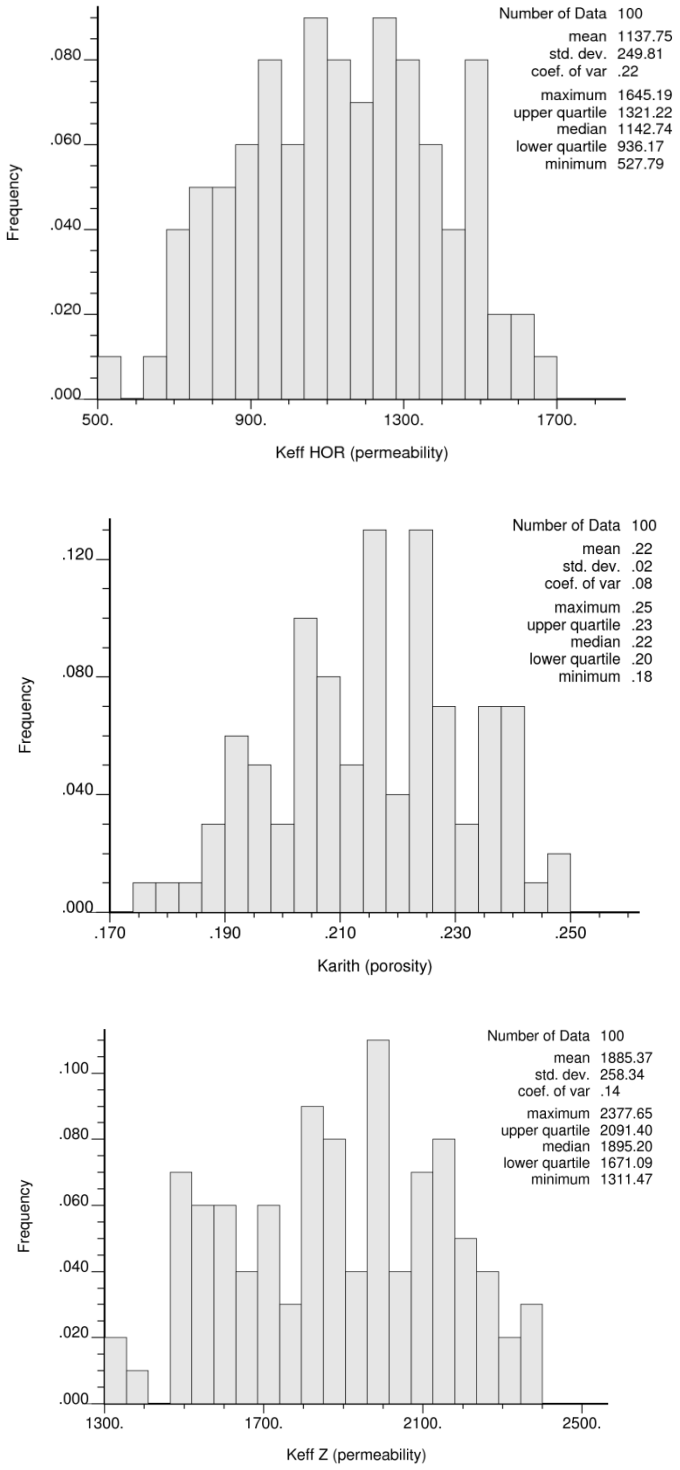

Fig. 20. Histogram of effective horizontal and vertical permeability values and arithmetic average of porosity

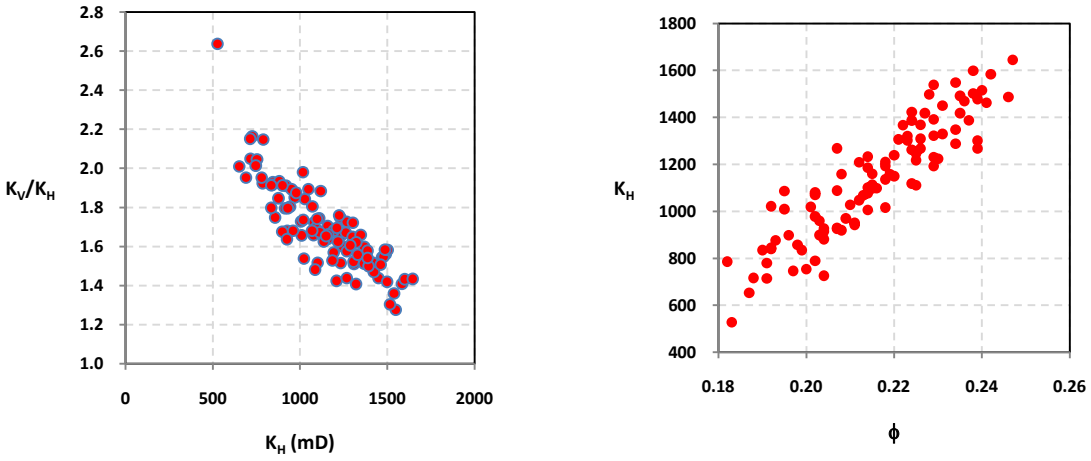

Fig. 21. Results for the K_V/K_H ratio versus the horizontal permeability (ρ=-0.85) and porosity versus horizontal permeability (ρ=0.91).

4. Regional modeling

Macro modeling is a tool for studying general properties of a reservoir or mine in macro scale. The total amount of bitumen/ore and its distribution over the region are of the great interest in macro modeling. In addition, it is interesting to know the distribution of uncertainty and to have optimistic and pessimistic estimates on the reservoir.

McMurray formation is one of the largest oil reservoirs in the world which is estimated to contain 180 billion barrels. This formation is located in north-east Alberta and covers a region of 120 by 180 kilometers approximately. Estimating the amount of bitumen in the formation and its properties and distribution over the region is the main goal of this section. This estimation can then be used for deciding on methods and requirements of the extraction and refinery processes.

The project is defined with the following steps: 1) initial data processing 2) studying preliminary stats 3) model building 4) post processing and reporting the results. .

4.1. Initial data processing

Like any other engineering practice, the available data provided by human or machines should be preprocessed. This preprocessing step contains tasks taken in order to clean the data, verify its consistency and prepare it for further studies. The data provided is obtained from a web database containing logs and histories of the wells placed in the McMurray formation. The first step is to clean data from invalid records. Duplicate values, null values and outliers are the most famous types of invalid records. Unfortunately, in our dataset null values are replaced with zeros which force us to make a decision on how to treat them. Consequently, there are two assumptions on zero values: first is that no data is collected from the well (null values) or the data was not enough reliable to be published and the second type is representing wells where no McMurray were present and the real values are zero.

In order to deal with these invalid records with zero values, the following approach has been taken. Wells with zero values where another non-zero record is present at the same location are eliminated from the set. Remaining zeros are considered as no McMurray which can be verified using location maps. There are other wells which are considered as no McMurray despite the fact that they have non-zero values. Records with a net thickness of less than or equal to 2 meters or with a mass

fraction of bitumen of less than or equal to 0.05 are considered as now McMurray present. These non-zeros are so small that it is not economical to consider them as in bitumen and also there may be some measurement errors in them. Fig. 22 shows the distribution of wells with the presence and absence of McMurray formation.. Black dots stand for well which have not shown considerable values. Table 9 represents the summary statistics of indicators. The next variable defined is calculated as multiplication of net thickness and mass fraction of bitumen used for further cross checks on the total amount of bitumen present in the region.

Table 9. Indicator variable summary

Number of 1	Number of 0	Mean	Standard deviation	Variance
2280	234	0.9069	0.2905	0.0844

Dealing with duplicates is the next step of data cleaning. An optimistic decision has been made and records with higher values are selected whenever duplicated data occurs.

The initial datasets contains 6839 records but only 2513 records remained after the data cleaning process. The other change required to be done is to clip the coordinates to be easier to work with. The UTM coordinates in the original data goes from 6095314.34 to 6417698.17m in North direction and from 375724.5 to 547494.18m in east direction. In order to have better looking coordinates, 6000000 and 300000 units have been subtracted from Y and X values respectively.

We are not usually interested in an exactly rectangular area in regional modeling. Therefore, the model is usually needed to be clipped to avoid misrepresentation of data and biased results. This clipping is done by an application called “ClipGrid.exe”. This application clips generated grids using a set of vertices provided in the parameter file. The vertices can be introduced by pairs of points. In order to find these border points easily an application called “DigXY.exe” is used. The program can open a bitmap of the region and save points selected by the user as the digitization result. In this case, the area is digitized using 100 points trying not to leave any well with McMurray formation present outside the clipped area.

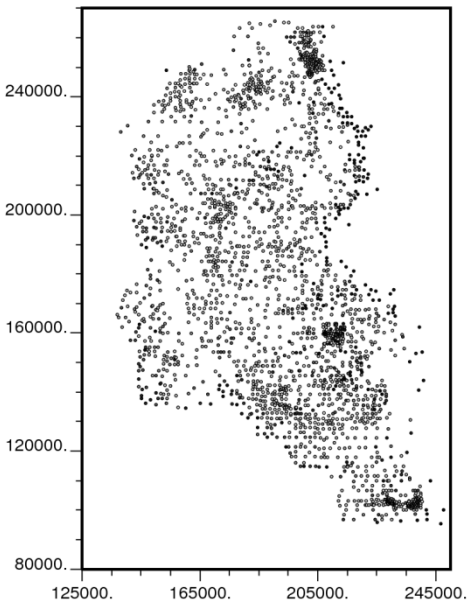

Fig. 22. Indicator map

In order to have a better understanding of the available well data, there seems to be a need to do some preliminary statistical studies on the data. There are four important variables to study. The first one is an indicator variable defined to distinguish wells with and without significant McMurray formation as defined in the previous section. This indicator has a value of 1 for 2280 records among the 2513 wells with valid data. The next variables of interest are the gross and net thickness of the formation and the mass fraction of bitumen. The histograms of these variables are shown in Fig. 23 to Fig. 25. As can be seen in the histograms there are still some zeros in different variables which show wells with no McMurray formation is present.

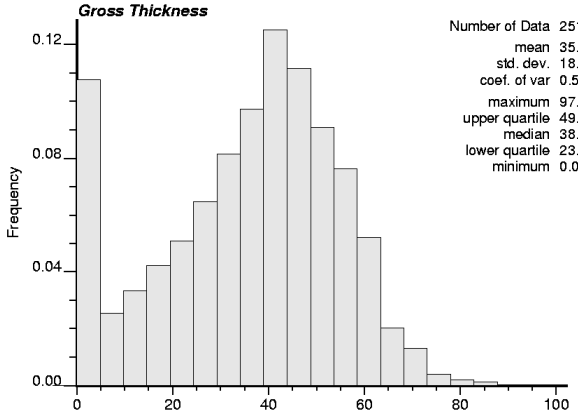

Fig. 23.Gross Thickness of Formation

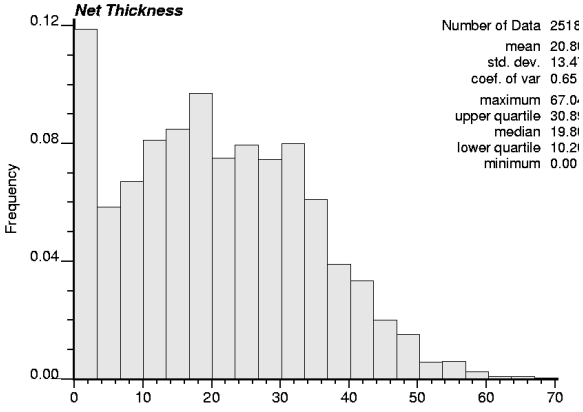

Fig. 24.Net Thickness of Formation

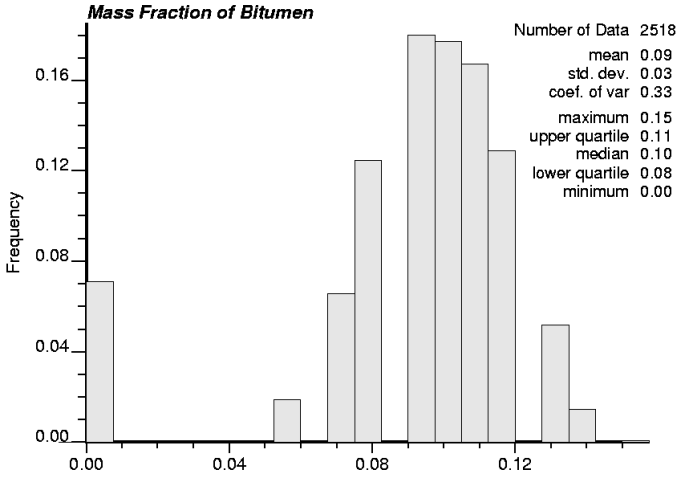

Fig. 25.Mass Fraction of Bitumen

4.1.5 Kriging indicator variable

After mapping the indicator variable and finding the borders of the area it seems reasonable to Krig the variable and clip it using the boundaries defined to examine the goodness of the borders and their relation with the probability of having bitumen inside and outside the boundaries. Kriging is one of the most important traditional mapping applications and an essential component of geostatistical simulation methods. In this part, a model of spatial uncertainty characterizing the distribution and occurrence of the indicator variables is constructed. There are 2514 data points that should be used to estimate unsampled locations that are inside the domain. In this case, the simple

Kriging was done using the given variogram model. In the given model, nugget effect is equivalent to 10 to 20 percent of sill and range is equivalent to a third of area dimension. Thus, nugget effect and range are equal to 0.017 and 70000, respectively. For Kriging 325×475 grid nodes were used. Size of each cell in X and Y directions are 400 m and 400 m, respectively. Fig. 26 shows a 2D view of Kriging result using indicators. Fig. 27 shows the Kriging result after applying the desired area.

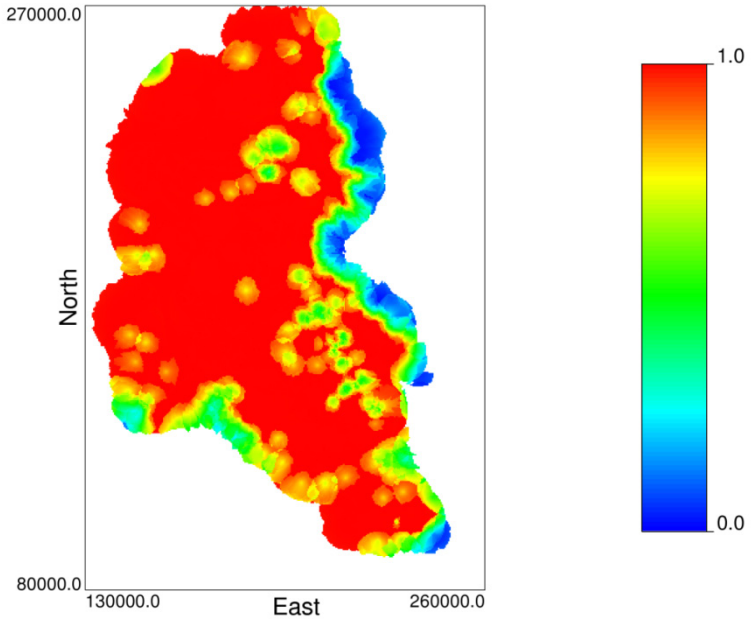

Fig. 26**.** Kriging result according to the indicators (Values less than zero has been trimmed)

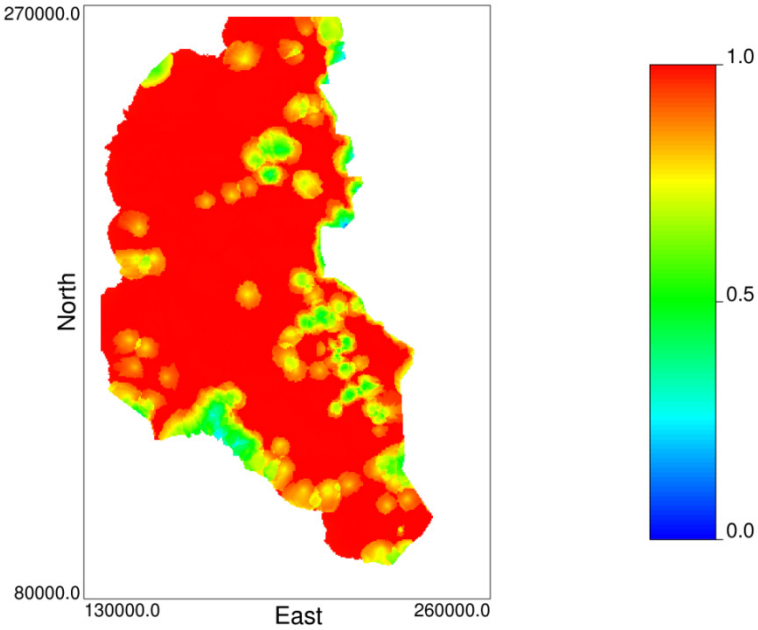

Fig. 27. Kriging result after clipping the data which are not in McMurray formation

4.1.6 Preliminary statistics

Wells are often drilled in areas with a greater probability of good reservoir rock. Closely spaced data inform fewer grid nodes and, hence, receive lesser weight. Widely spaced data inform more grid nodes and, hence, receive greater weight (C.V. Deutsch, 2002). In this project, there are clustered data in some areas. Fig. 28 shows location map of wells. It can be clearly seen in the right hand side of the map that there are three areas the wells are closer. The summary statistics were done under two different condition, equal weights and declustering weights.

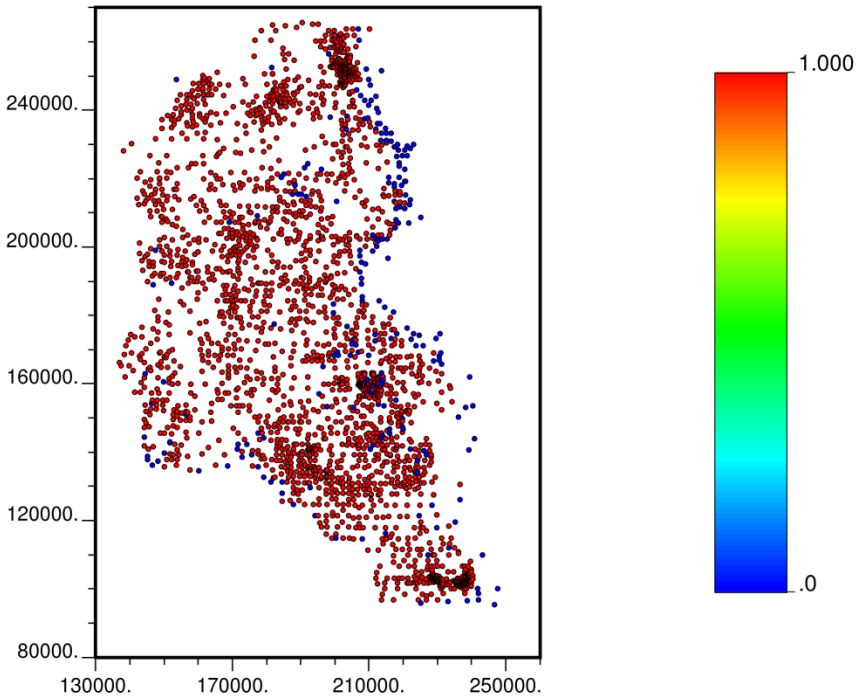

Fig. 28. Location map of the wells (The filled red circles belong to McMurray)

With declustering technique, a weight is assigned to each datum based on its closeness to surrounding data. Then the histogram and summary statistics are calculated with declustering weights. The technique of cell declustering is used in this project. For this purpose "declus.exe" program is used. The area of interest is divided into a grid of cells, then the occupied cells, and number of data in each of them is counted. Finally, weight of each data is calculated according to the number of data falling in the same cell. The summary statistics from declustering and equal weighted techniques for 2514 well data are shown in Fig. 30 and Table 10. The optimum cell size is determined automatically by "declus.exe" program. The plot of declustered mean versus cell size is shown in Fig. 29. A cell size of 16000 units with declustered mean of 16 was chosen.

The relationships between gross interval with net interval and net interval with average mass bitumen, with and without declustering were considered. Correlations between these variables have been compared in Table 11. It can be clearly seen that correlation of the cell declustering is more than equal weighted.

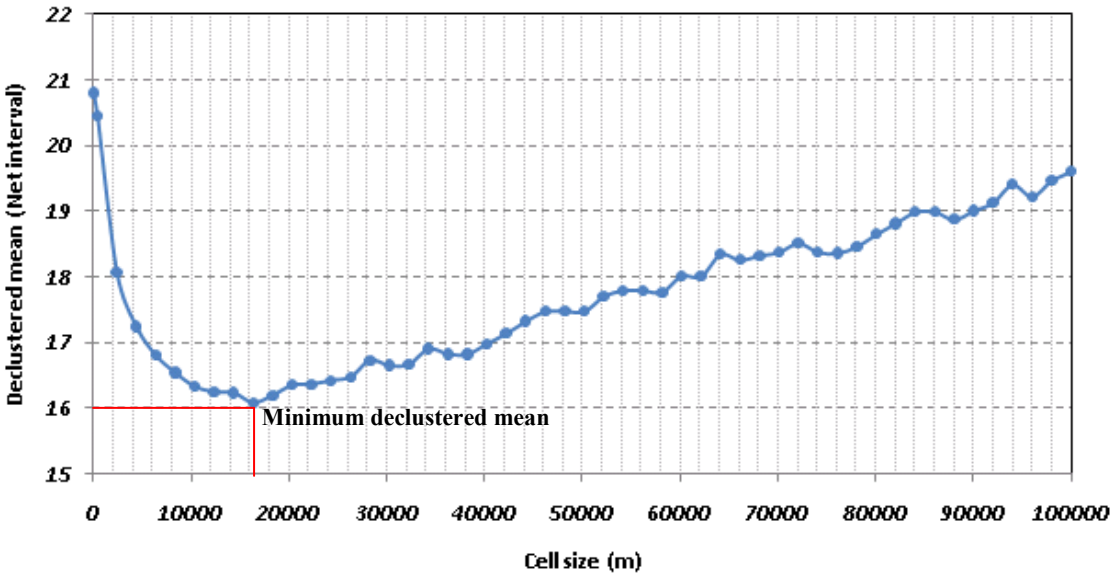

Fig. 29. Declustered mean versus cell size for Net interval

Table 10.Summary statistics of 2514 well data

	Minimum	Maximum	Mean		Standard deviation	
			Equal weighted	Cell declustering	Equal weighted	Cell declustering
Gross Interval (m)	0	97.5	35.78	29.17	18.81	19.58
Net Interval (m)	0	67.04	20.80	16.08	13.47	13.01
Average mass Bitumen (% Mass)	0	0.15	0.09	0.08	0.03	0.04

Table 11.The comparison of correlations between equal weighted and cell declustering

	Equal weighted	Cell declustering
Gross-Net (m)	0.804	0.825
Gross-Bitumen (m)	0.668	0.696

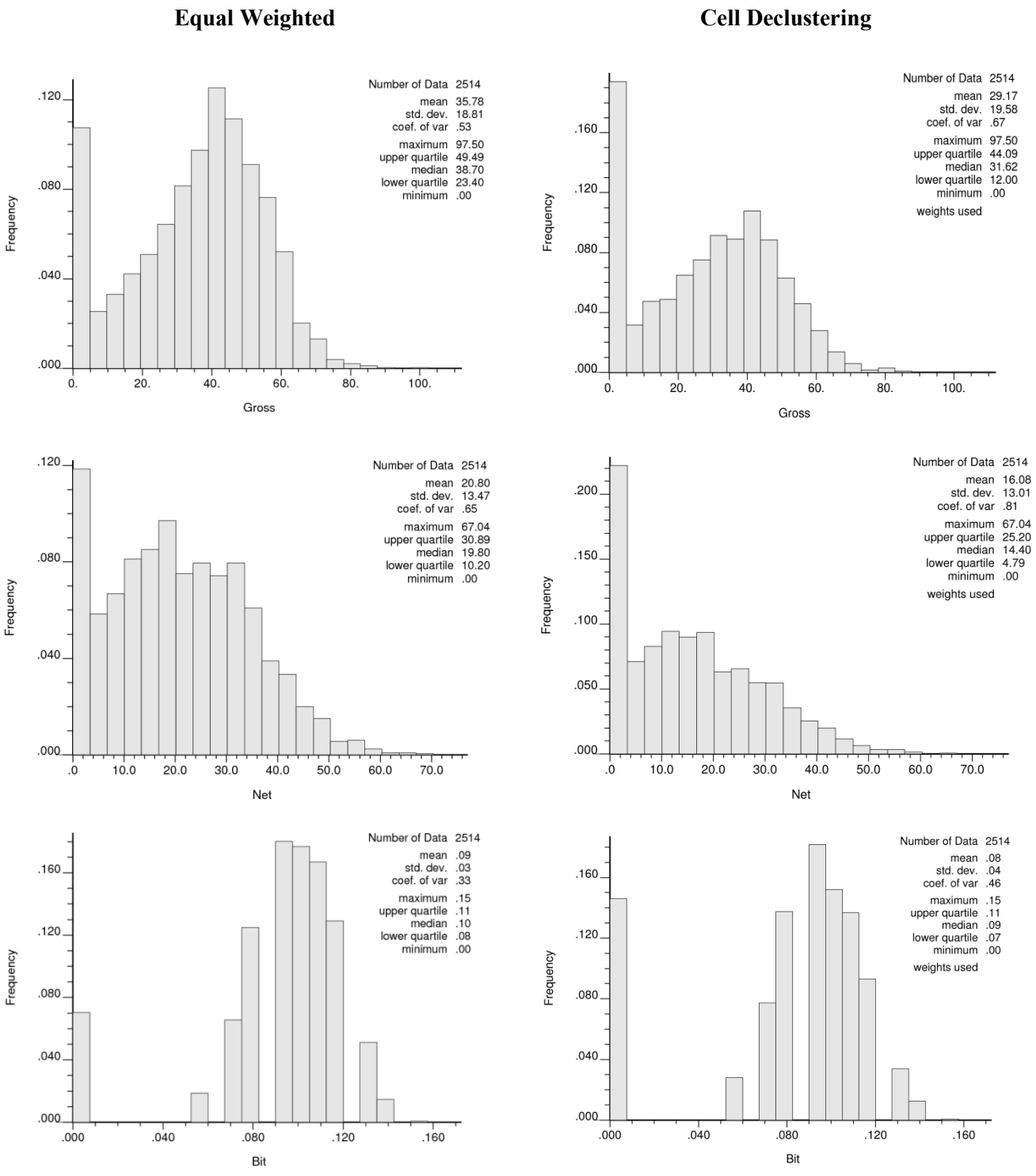

Fig. 30**.** Histogram of Gross interval, Net interval and Average mass of Bitumen with and without weight.

For estimating the amount of Bitumen in area of interest, regional area should be calculated. For this purpose, points from output of "DigXY.exe" are used and polygon area from joining the points is calculated using "Polyar.exe" program. The area of study is equal to 10.2×10^7 Km^2. To calculate the amount of Bitumen in the area of interest, Eq. (3) is used.

$$A\times\overline{T}\times\overline{B}\times C \tag{3}$$

Where A is the area of interest, $\overline{T}$ is the average net thickness of oil sand, $\overline{B}$ is the average mass of Bitumen, and C is a convergence factor. Calculation is done according to Table 12. To calculate barrels of bitumen the average net interval after declustering is used.

Table 12.Calculation of amount of Bitumen in study area

# of row	Description	Unit	formula	Value
(1)	Area	m^2	----------	10,232,151,394.4
(2)	$\overline{T}$	m	----------	16.1
(3)	$V_{Oil\,sand}$	m^3	(1)×(2)	164,532,994,421.1
(4)	$Density_{Oil\,sand}$	Kg/ m^3	----------	2,160.0
(5)	$Mass_{Oil\,sand}$	Kg	(3)×(4)	355,391,267,949,680.0
(6)	$\overline{B}$	Fraction	----------	0.0822
(7)	$Mass_{Bitumen}$	Kg	(5)×(6)	30,063,156,915,864.6000
(8)	$Density_{Bitumen}$	Kg/ m^3	----------	1,050.0
(9)	$V_{Bitumen}$	m^3	(7)/(8)	27,808,520,547.4
(10)	**Note:** 0.159 m^3 is equal to 1 bbl			
(11)	Bbl of Bitumen	------	(9)/(10)	174,910,656,515.2

4.2. Calculating the variogram

The variogram is function of distance and direction. Variogram inference proceeds in three main steps (Leuangthong, et al., 2008):

1. Calculate the experimental variogram in multiple directions for a number of lags that approximately correspond to the average spacing between data,
2. Interpret the experimental variogram points and supplement them with expert judgment or analogue data,

3. Fit a valid parametric model to the directional variograms in all directions.

Variogram maps are first generated to find the direction of continuity in the area. Variogram maps are presented in Fig. 31.

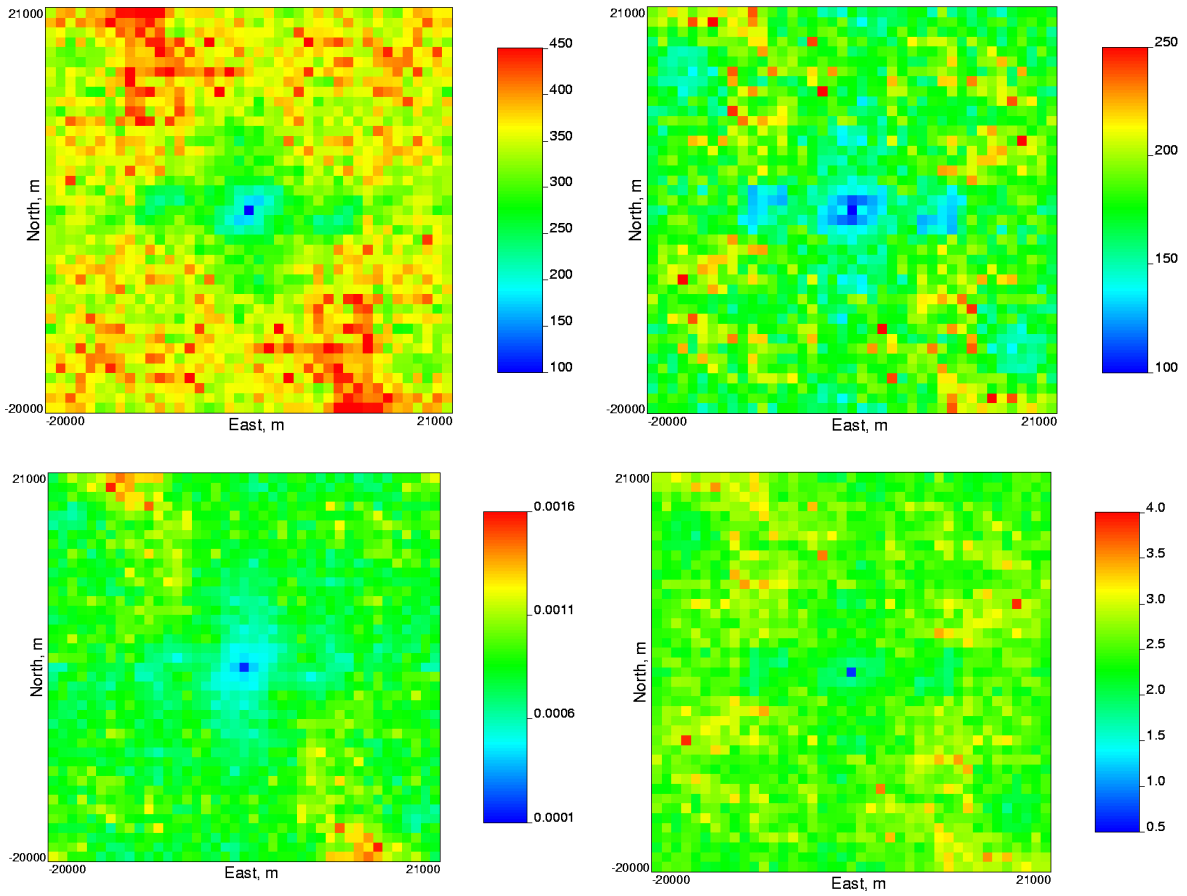

Fig. 31. Variogram maps for gross and net thickness, mass fraction of bitumen and bitumen per area

Looking at the variogram maps, an azimuth of 150 degrees south-east seems to be the direction of continuity but calculating experimental variograms they happened to have almost the same variogram range in the mentioned direction and an orthogonal one. Therefore, a horizontal variogram is used instead of a directional one for all variables.

Different variogram models have been tested by accuracy plots and cross validation in Kriging. The best resulting variogram models (based on try and error) and the corresponding accuracy plots and cross validation scatter plots are shown in the following parts.

In this part, variograms of gross interval, net interval, and bitumen were calculated. In subsequent steps such as Kriging and simulation, we need a parametric variogram model, which is fitted to the experimental points.

Gross interval

For gross interval, three variance regions can be defined as shown in Eq. (4). The first one is a nugget effect; the second one is exponential variogram structure. The last one is spherical variogram structure.

$$\gamma(h) = 0.1 + 0.87\, Exp_{\substack{a_{h\max}=10000 \\ a_{h\min}=10000}}(h) + 0.03\, Sph_{\substack{a_{h\max}=60000 \\ a_{h\min}=60000}}(h) \tag{4}$$

Net interval

For net interval, also three variance regions like as gross interval can be defined as in Eq.(5).

$$\gamma(h) = 0.1 + 0.85\, Exp_{\substack{a_{h\max}=8000 \\ a_{h\min}=8000}}(h) + 0.05\, Sph_{\substack{a_{h\max}=50000 \\ a_{h\min}=50000}}(h) \tag{5}$$

Average mass Bitumen

This variable also has variance regions as same as two other variables. Eq.(6) presents the variogram for average mass bitumen.

$$\gamma(h) = 0.3 + 0.45\, Exp_{\substack{a_{h\max}=16000 \\ a_{h\min}=16000}}(h) + 0.25\, Sph_{\substack{a_{h\max}=3200 \\ a_{h\min}=3200}}(h) \tag{6}$$

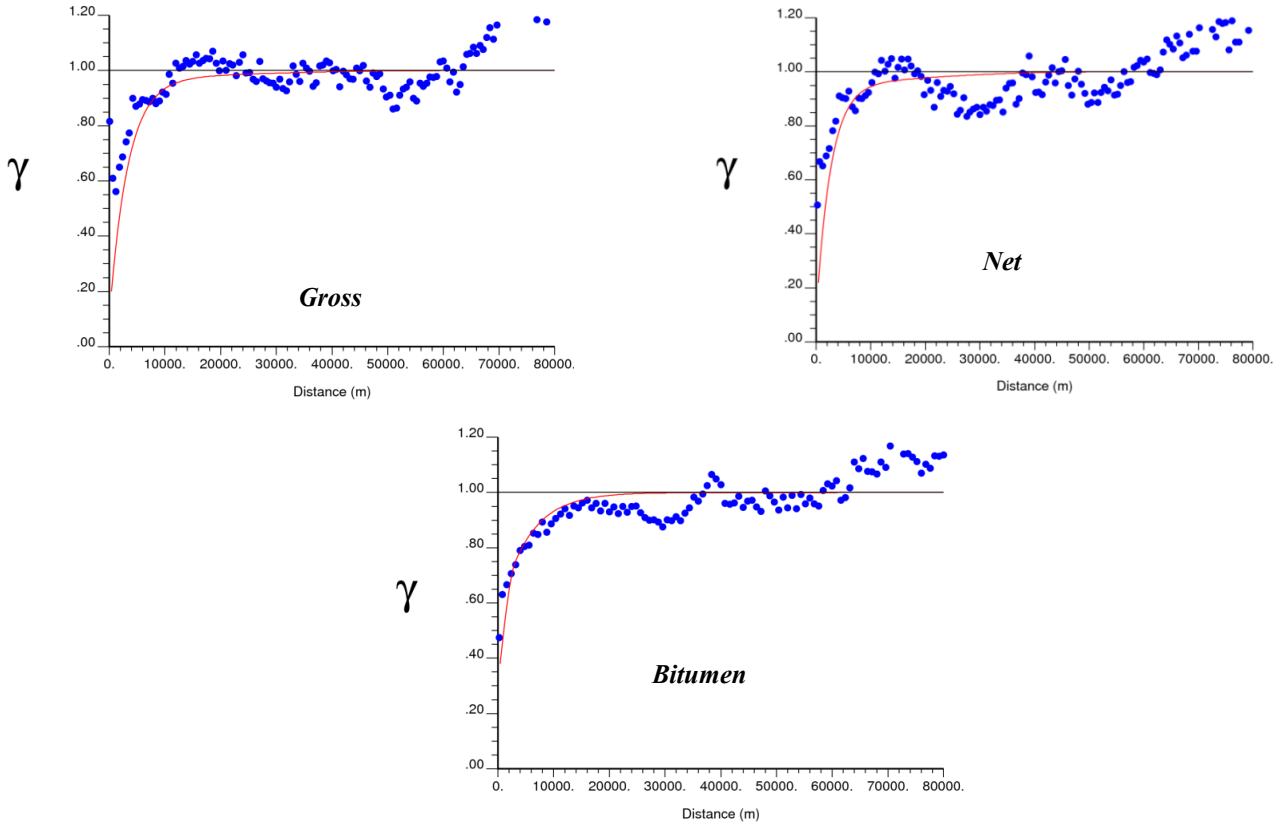

Fig. 32.The variogram models of gross interval, net interval, and average mass Bitumen

The variogram parameters corresponding to variogram shown in Fig. 31 have been summarized in Table 13.

Table 13.Variogram parameters corresponding to variograms shown on **Fig. 32**

Variable	Variance Contribution	Type of Variogram	a_{hmax}, a_{hmin}, m
Gross interval	0.1	Nugget	
	0.87	Exponential	10000
	0.03	Spherical	60000
Net interval	0.1	Nugget	
	0.85	Exponential	8000
	0.05	Spherical	50000
Average mass Bitumen	0.3	Nugget	
	0.45	Exponential	16000
	0.25	Spherical	3200

4.3. Bootstrap for uncertainty in mean

Bootstrap is a method developed by Efron. The Monte Carlo simulation is applied in this method. It is a statistical resampling technique which permits quantification of uncertainty in statistics by resampling from the original data. With this method, the uncertainty in input statistics is known. The histograms at the right hand side of Fig. 33 show the uncertainty in the mean of variables for 5000 realizations. The spatial bootstrap was applied to arrive at the distribution of uncertainty in the mean of each input variable. It can be seen that the mean of gross interval, net interval, and average mass Bitumen remain unchanged.

4.4. Trend map

The trend map is used to provide the overall trend of each variable in the entire study area. This map is created by simple Kriging with a variogram designed to reveal large scale features. Usually, a long range variogram with modest nugget effect is used (Ren, et al., 2006) .

In this case, the simple Kriging was done using the given variogram model. In the given model, nugget effect is equivalent to 30 percent of sill and range is equivalent to a third dimension area. Thus, nugget effect for gross interval, net interval, and average mass Bitumen are considered equal to 106.14, 54.43, and 0.00027, respectively. For Kriging 325×475 grid nodes was used. Size of each cell in X and Y directions are 400 m and 400 m, respectively. The trend maps of gross interval, net interval, and average mass bitumen are shown in Fig. 34. Table 14 shows comparison between the results of trend map and cell declustering. The percentage of difference between results of trend map and declustering for all variables is more than expected value. This difference should be around 5 percent, but here minimum difference is around 12.5 percent.

4.5. Model building

4.5.1 Estimation

In this step variogram models are tested to see how good they fit the data. To do so, a Kriging operation is done on the normal score transformed data. The only difference is that instead of Kriging the cell, data locations are Kriged. These values are then plotted against their true value to see how good they are. Fig. 35 shows the cross plot of true versus estimate for each variable. The

correlation of gross interval, net interval and average mass Bitumen are 0.626, 0.632 and 0.568, respectively.

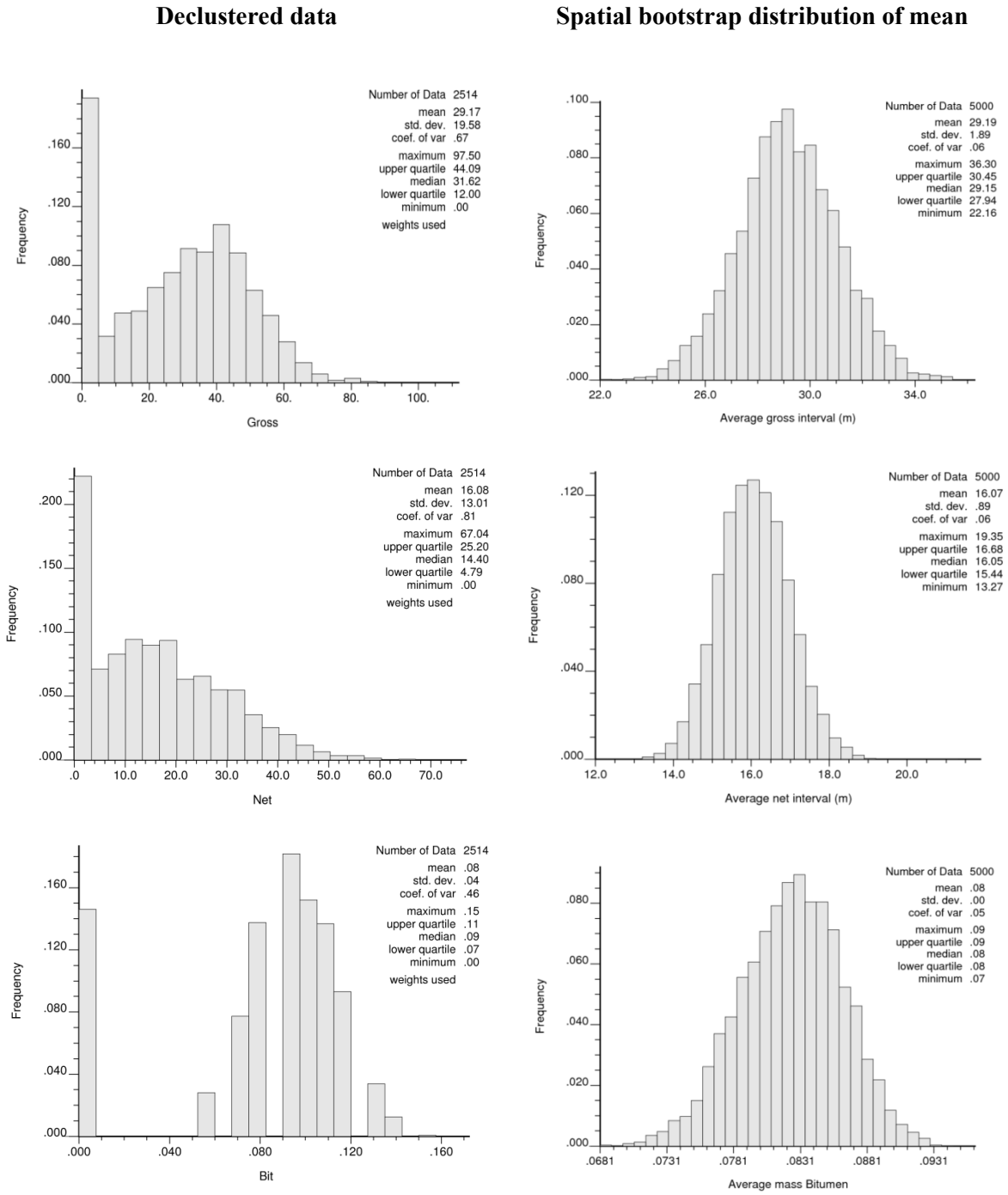

Fig. 33**.** Histogram of 2514 data for gross, net, and bit after cell declustering are shown at left hand. Histogram of spatial bootstrap results to show the distribution of uncertainty in the mean of each variable are shown at right hand.

Table 14.The comparison between average of the clipped trend model and declustered

	Average		Difference (%)
	Trend map	Cell declustering	
Gross interval (m)	33.37	29.17	14.4
Net interval (m)	18.27	16.08	13.62
Average mass Bitumen (%Mass)	0.09	0.08	12.5

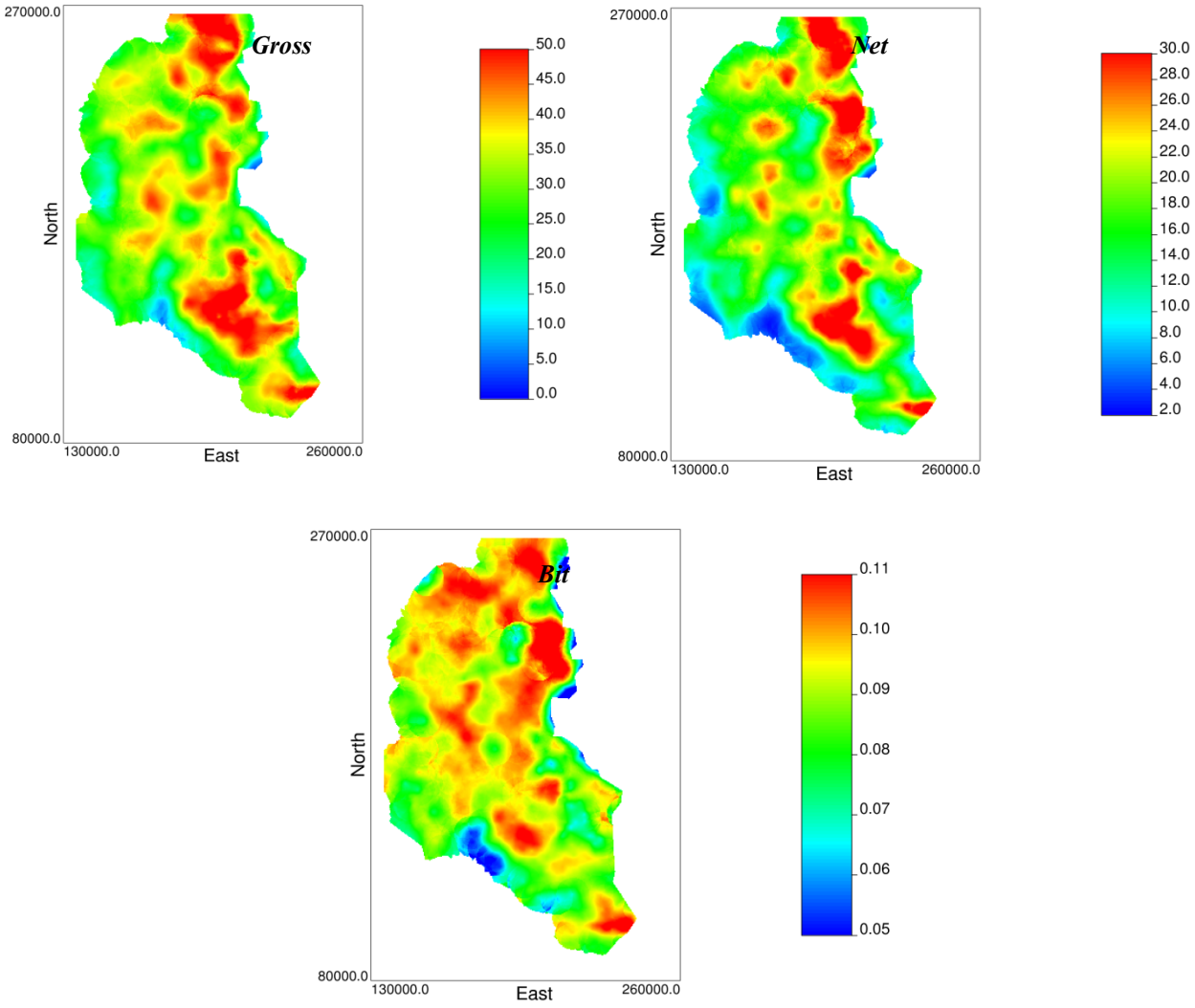

Fig. 34.The trend maps of gross interval, net interval, and average mass Bitumen

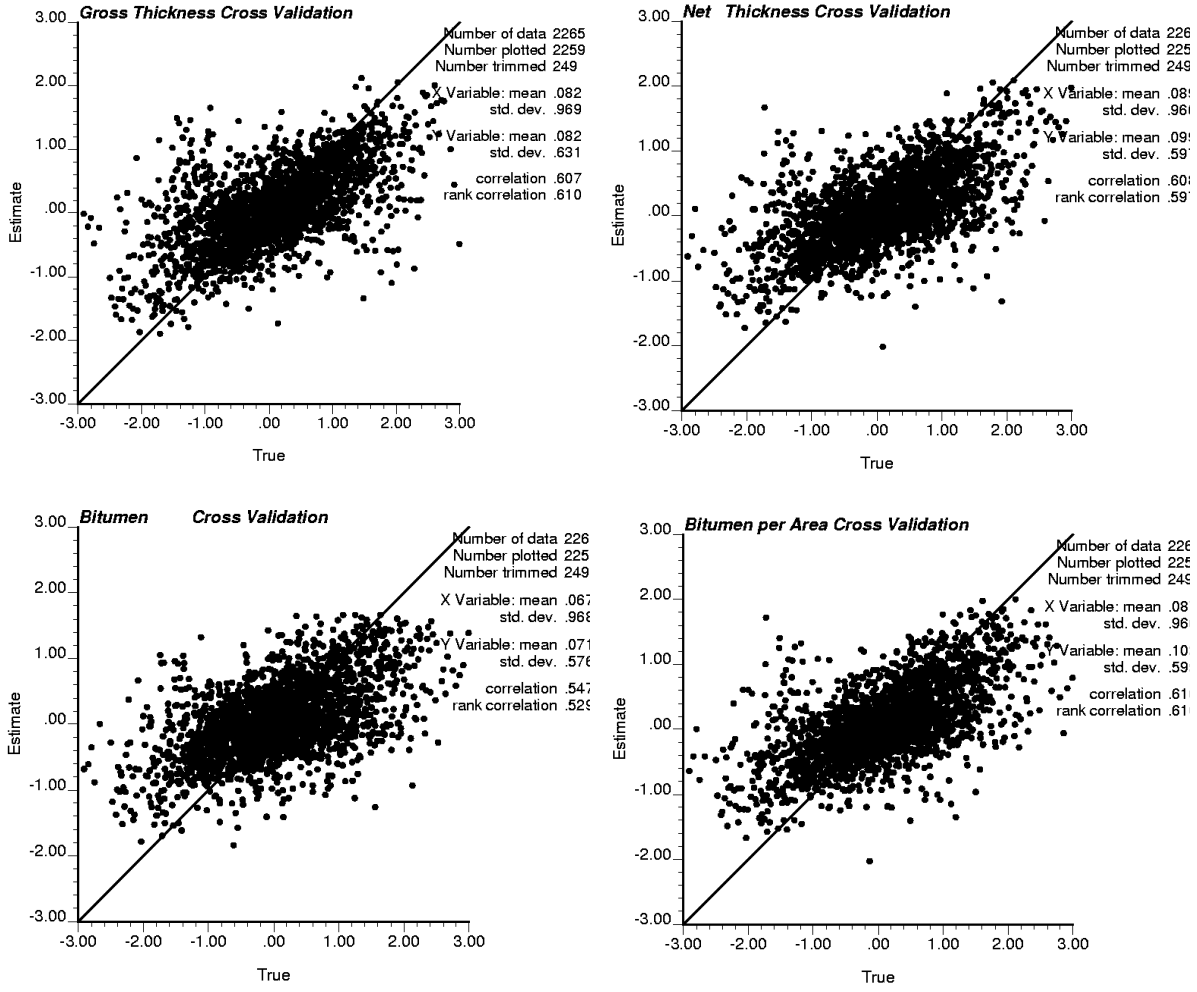

Fig. 35.Cross plot of true values versus estimated values for gross and net thickness, mass fraction of bitumen and bitumen per area

Another method used for cross validation is plotting the histogram of estimate versus true. This histogram should have a mean close to zero and a symmetric shape. Fig. 36 shows this histogram for the each variable.

Location map of error for each variable is also used for cross validation. Location map of error for gross and net intervals are shown in Fig. 37. It can be seen that the distribution of plus and minus signs approximately are same and that means there is no bias.

In the context of evaluating the goodness of a probabilistic model, specific definition of accuracy and precision are proposed. For probability distribution, accuracy and precision are based on the actual fraction of true values falling with in symmetric probability intervals of varying width *p* (C.V. Deutsch, 2002):

- A probability distribution is accurate if the fraction of true values falling in the *p* interval exceeds *p* for all *p* in [0, 1].
- The precision of an accurate probability distribution is measured by the closeness of the fraction of true values to *p* for all *p* in [0, 1].

A graphical way to check the accuracy is to cross plot actual proportion versus probability interval and see that all of the points fall above or on the 45^{o} line.

The results are ideal if the points fall close to the 45 degree line. The distribution of uncertainty are too wide when the points fall above the 45 degree line and too narrow when the points fall below the 45 degree line. The range of spatial correlation can control the spread of the distribution of uncertainty. Cross plot of actual probabilities versus the predicted probabilities for each variable are shown in Fig. 38. The closeness of the results to the 45 degree line attest to the goodness of the probabilities. As it can see in Fig. 38 the closeness of the results to the 45 degree line for net interval and average mass Bitumen are better than gross interval.

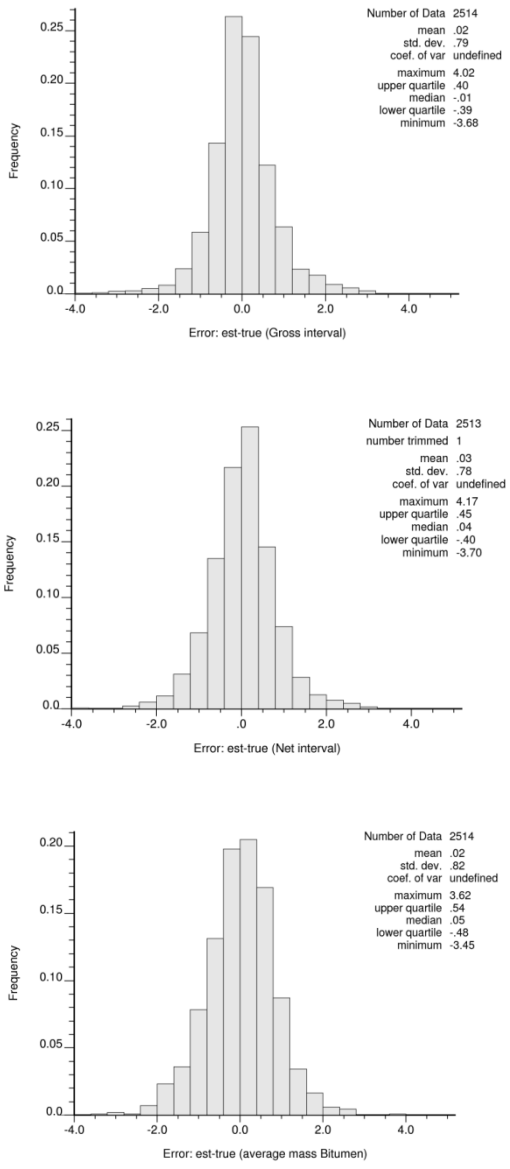

Fig. 36**.** Histogram of estimation minus true value for each variable

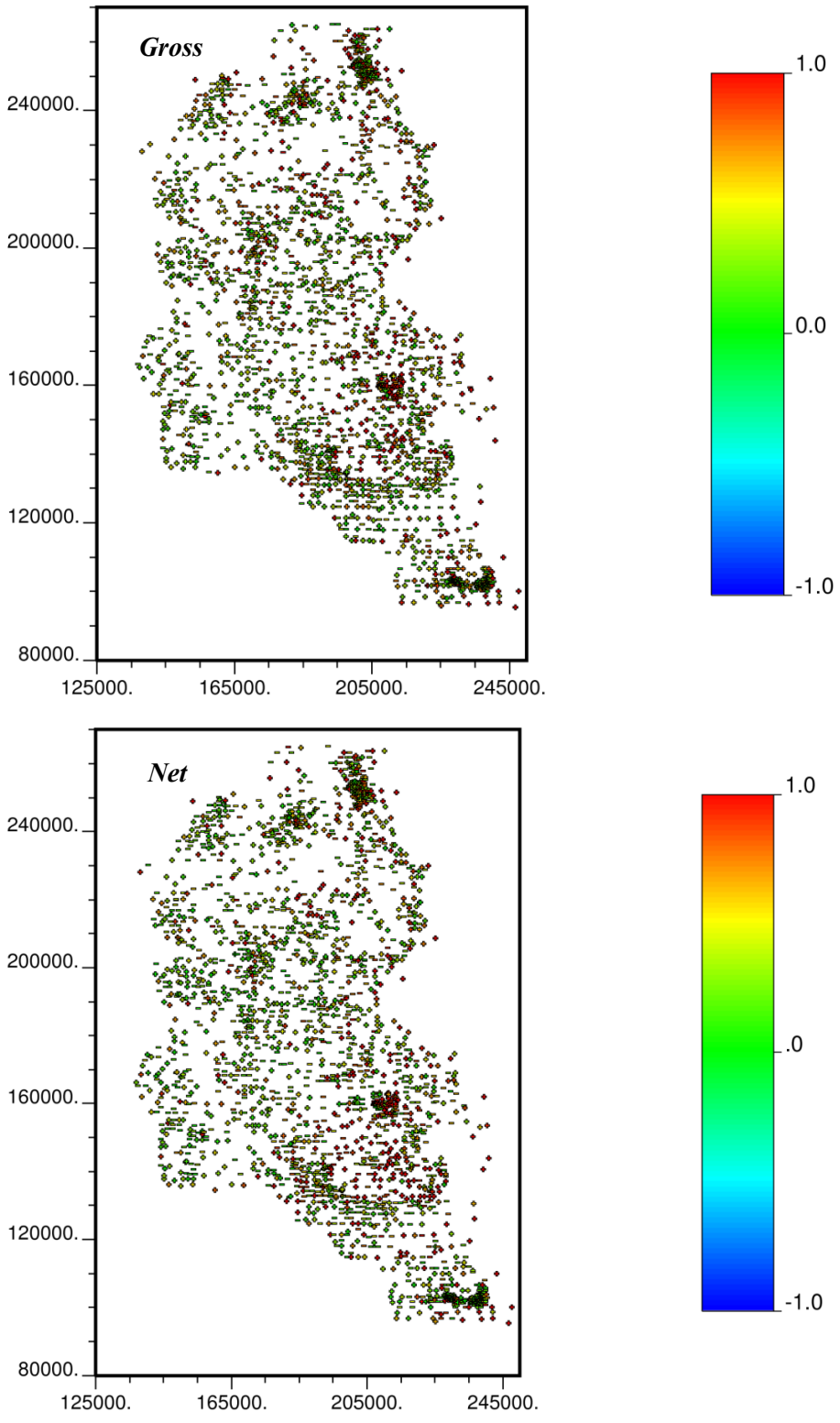

Fig. 37. Location map of estimation minus true value for gross and net intervals

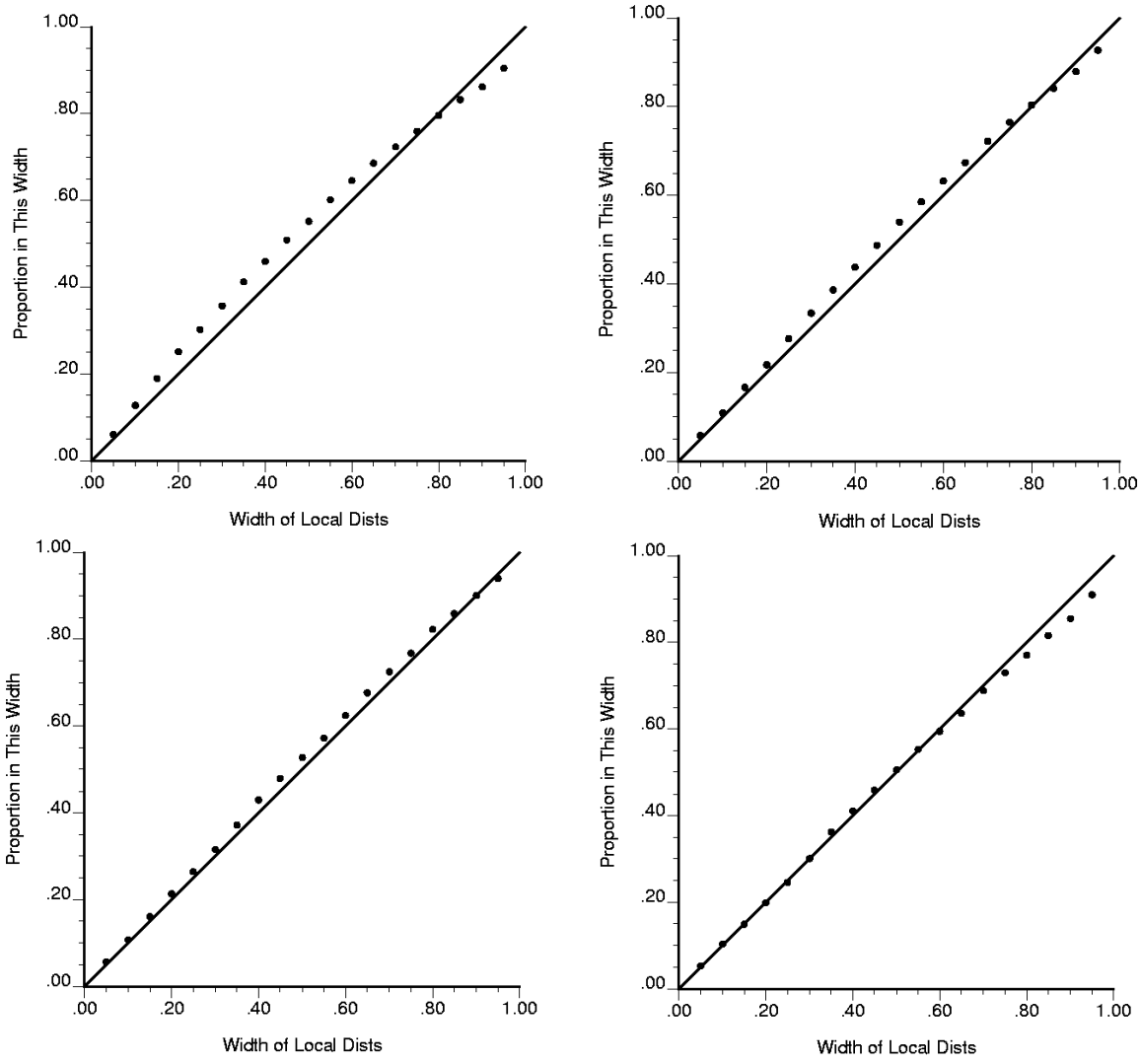

Fig. 38**.** Cross plot of actual probabilities versus the predicted probabilities for gross and net thickness, mass fraction of bitumen and bitumen per area

After cross validation, the Kriging was done for each variable. Kriging is one of the most important traditional mapping applications and an essential component of geostatistical simulation methods. In this case, Simple Kriging (SK) was done using the variogram model provided in Eqs. (4), (5), and (6). For Kriging 325×475 grid nodes was used. Fig. 39 shows the results of Kriging for each variable after clipping and transforming to the original unit.

The results of Kriging for each variable were back transformed to the original units. The results have been illustrated in Table 15.

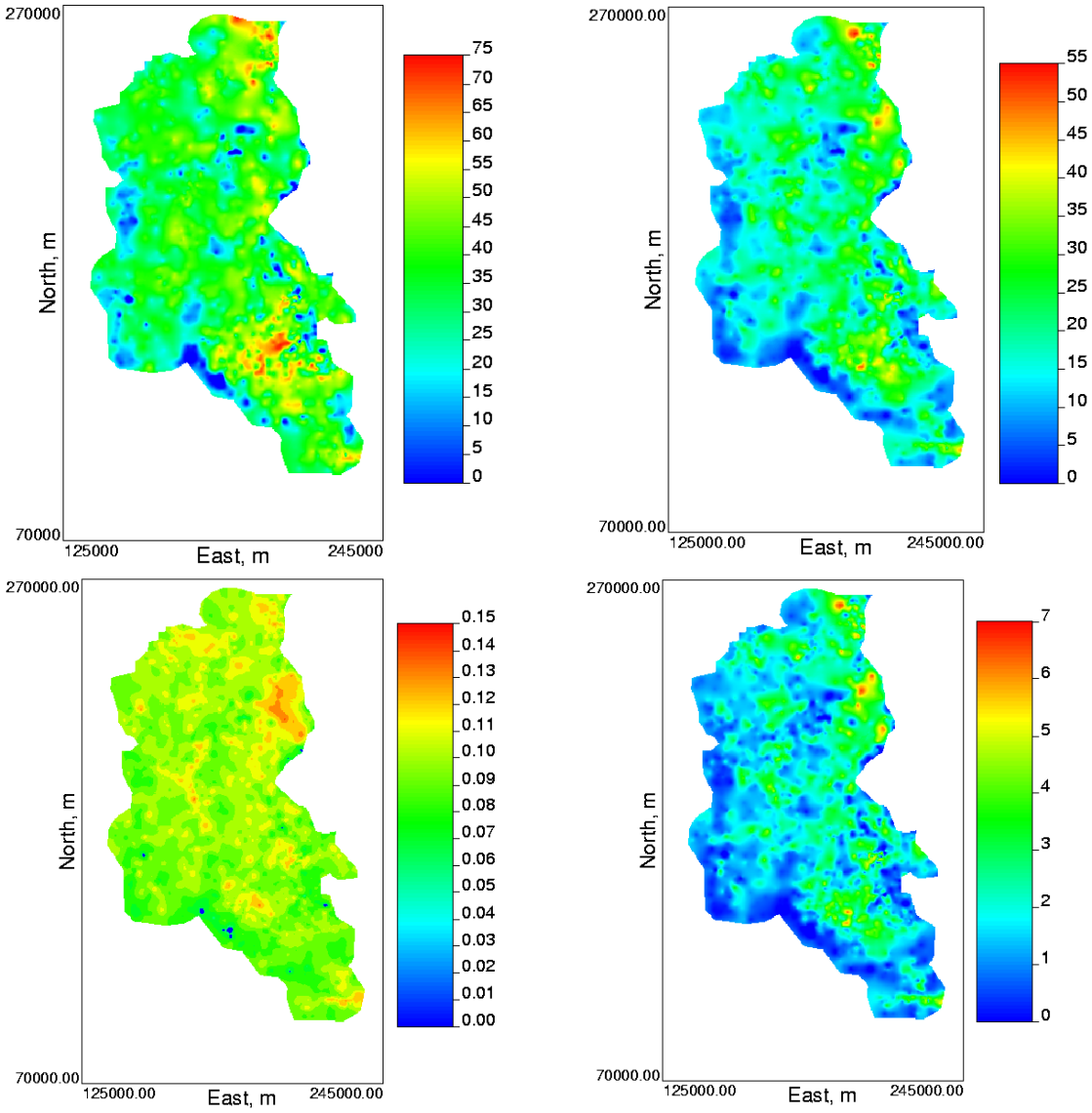

Fig. 39**.** Kriged map of different variables

Table 15**.**The results of kriging for each variable after back transforming

	Minimum	Maximum	Mean
Gross interval (m)	0	74	35.733
Net interval (m)	0	55.53	18.841
Average mass bitumen (% Mass)	0	0.14	0.0964
Bitumen per area (% Mass by m^2)	0	7.78	1.82

4.5.2 Simulation

Geostatistical realizations are being used increasingly for uncertainty quantification. In this case, for simulating, 325×475 grid nodes were used. To summarize and calculate the point-by-point average of the 100 realizations, "postsim.exe" program was used. The correlation between Kriging and simulation for gross interval, net interval, and average mass Bitumen in original units were 0.963, 0.972, and 0.853, respectively. An issue in here is the simulation of net thickness. In both simulation and Kriging there is a chance of having net thickness values higher than gross thickness. Note that in simulation it is more probable having such points. To deal with the inconsistency between net and gross thickness, net thickness is considered equal to gross thickness wherever it exceeds.

In addition to correlation between Kriging and simulation, the correlation between results of simulation and true values was calculated for each variable, all correlations were around 0.98.

The result of simulation for each variable has been illustrated in Table 16. The fluctuations of the realization variograms were also investigated. Fig. 40 shows variogram reproduction. The blue is the calculated variogram, yellow is average of simulated, and reds are 100 realizations. It can be seen that at the short distances, the variograms have been reproduced well.

To show uncertainty P_{10} and P_{90} values were used. The P_{10} represents there is a 90% probability of being larger than this value. It can also be used to identify the high value areas because when the P_{10} value is high then the value is surely high. The P_{90} represents there is a 90% probability of being less that this value. The P_{90} map can be used to identify the low valued areas because when the P_{90} value is low then the value is surely low.

The P_{10}, P_{90}, and P_{90}-P_{10} maps for gross interval, net interval and average mass Bitumen are shown in Fig. 41, Fig. 42, and Fig. 43, respectively.

Table 16.The results of simulation for each variable

	Minimum	Maximum	Mean
Gross interval (m)	0	90.6	33.49
Net interval (m)	0	67.04	18.71
Average mass bitumen (%Mass)	0	0.15	0.082
Bitumen per area (%Mass by m^2)	0	7.34	1.87

4.6. Comparison

In this section, the results of estimation and simulation are compared with true values. Fig. 44 shows comparison between true values and results of estimation and simulation. In addition, the amount of Bitumen according to the different methods has been summarized in

Table 17. It can be seen that the obtained results for amount of Bitumen from estimation and simulation are more than declustering.

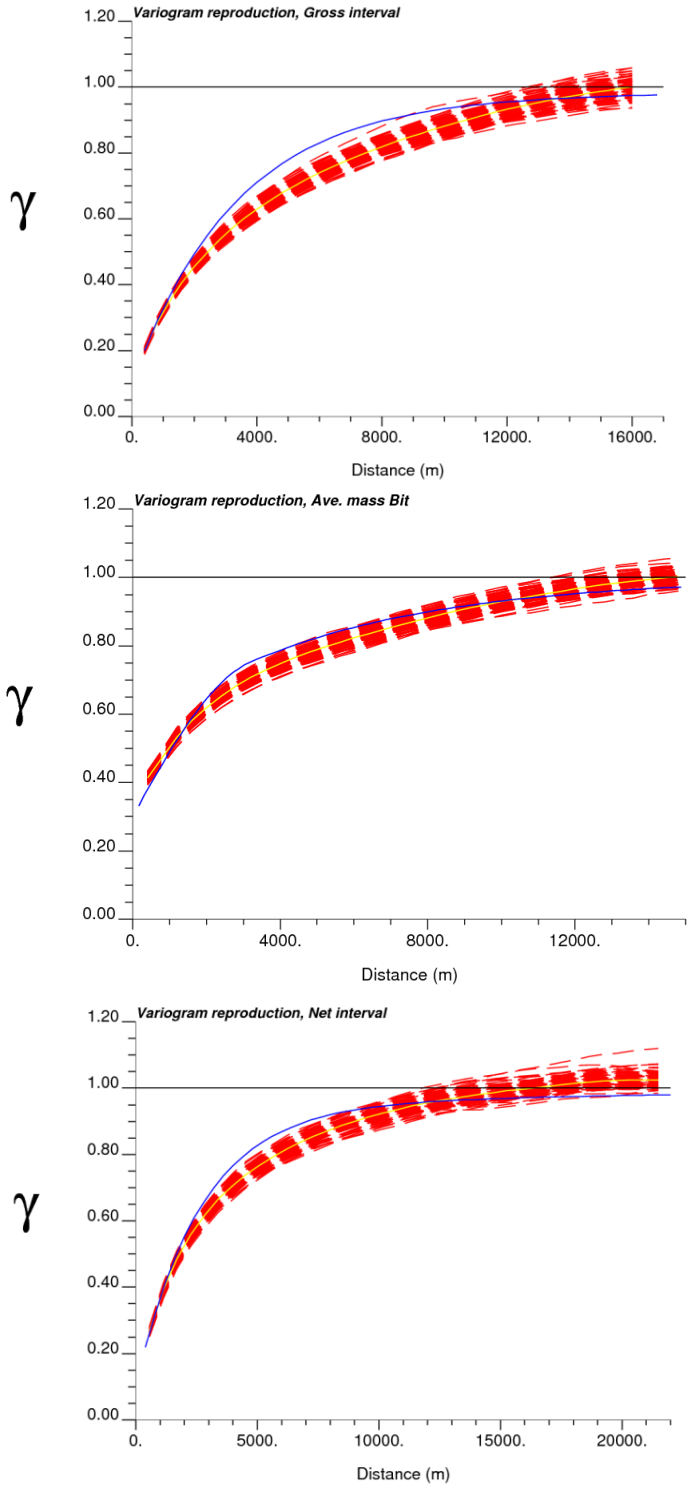

Fig. 40.Histogram and variogram reproduction (yellow line is the average variogram of 100 realizations and blue line is the calculated variogram)

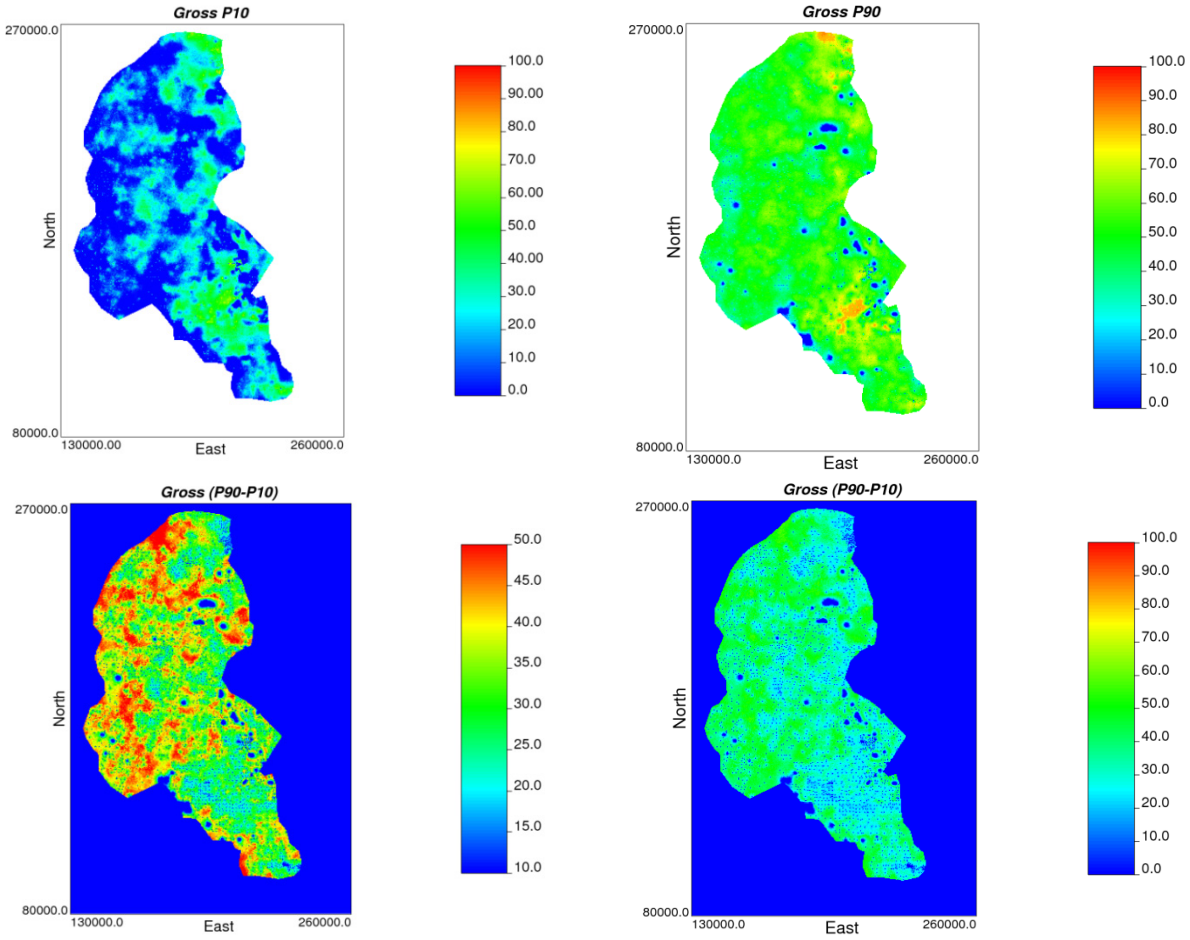

Fig. 41.The P_{10}, P_{90}, and P_{90}-P_{10} maps of gross interval

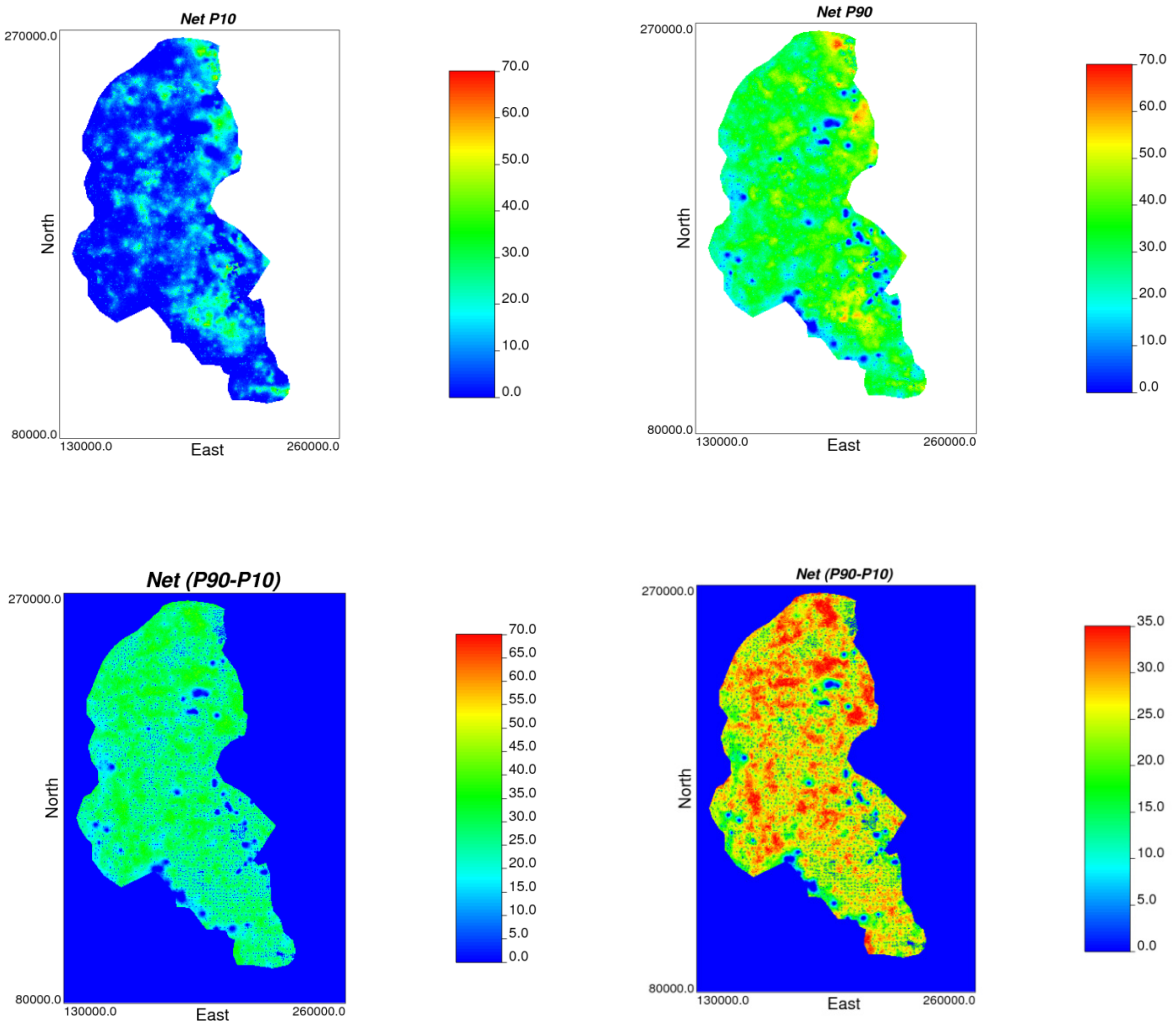

Fig. 42.The P_{10}, P_{90}, and $P_{90\text{-}P10}$ maps of net interval

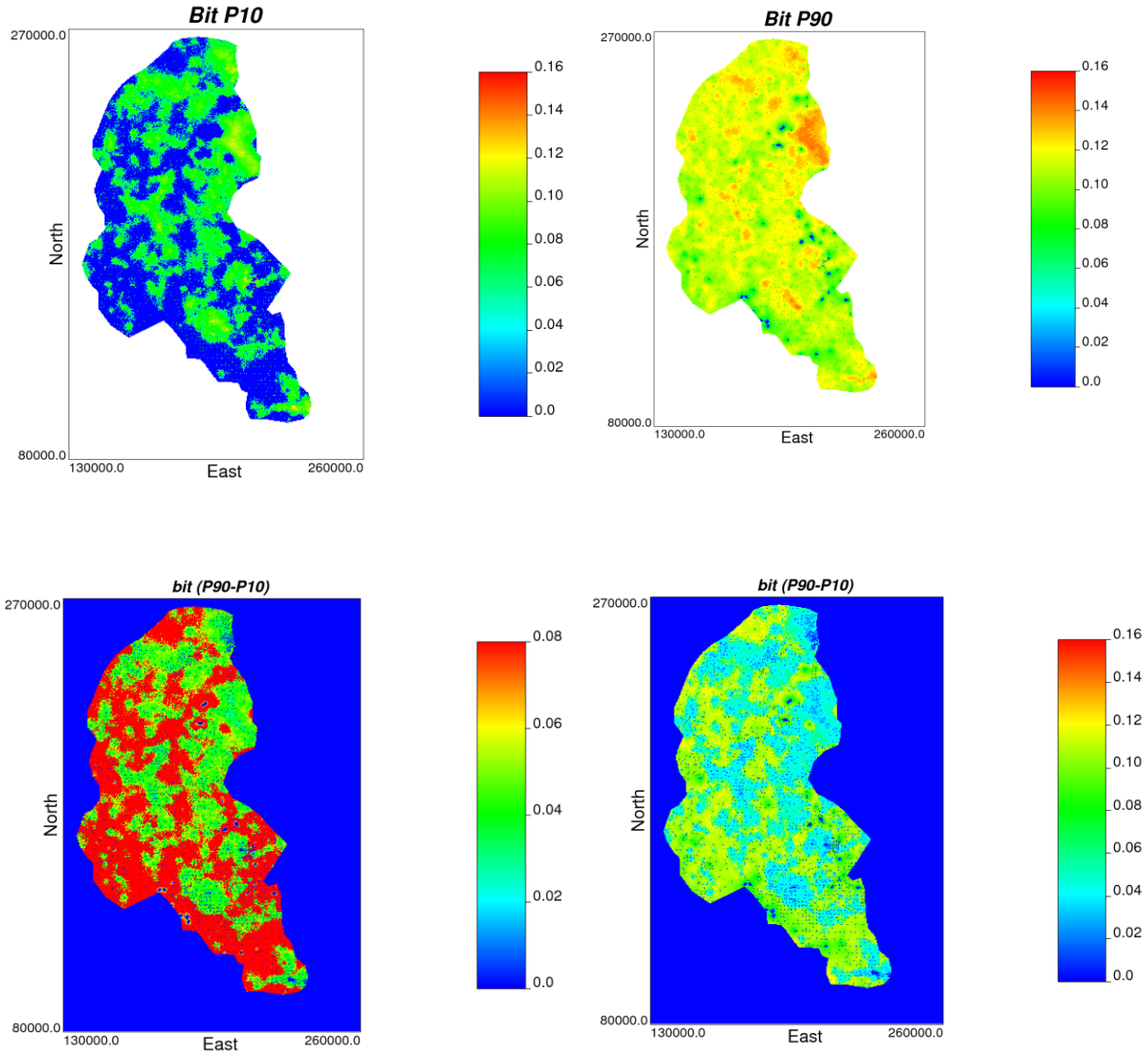

Fig. 43.The P_{10}, P_{90}, and $P_{90\text{-}P10}$ maps of average mass bitumen

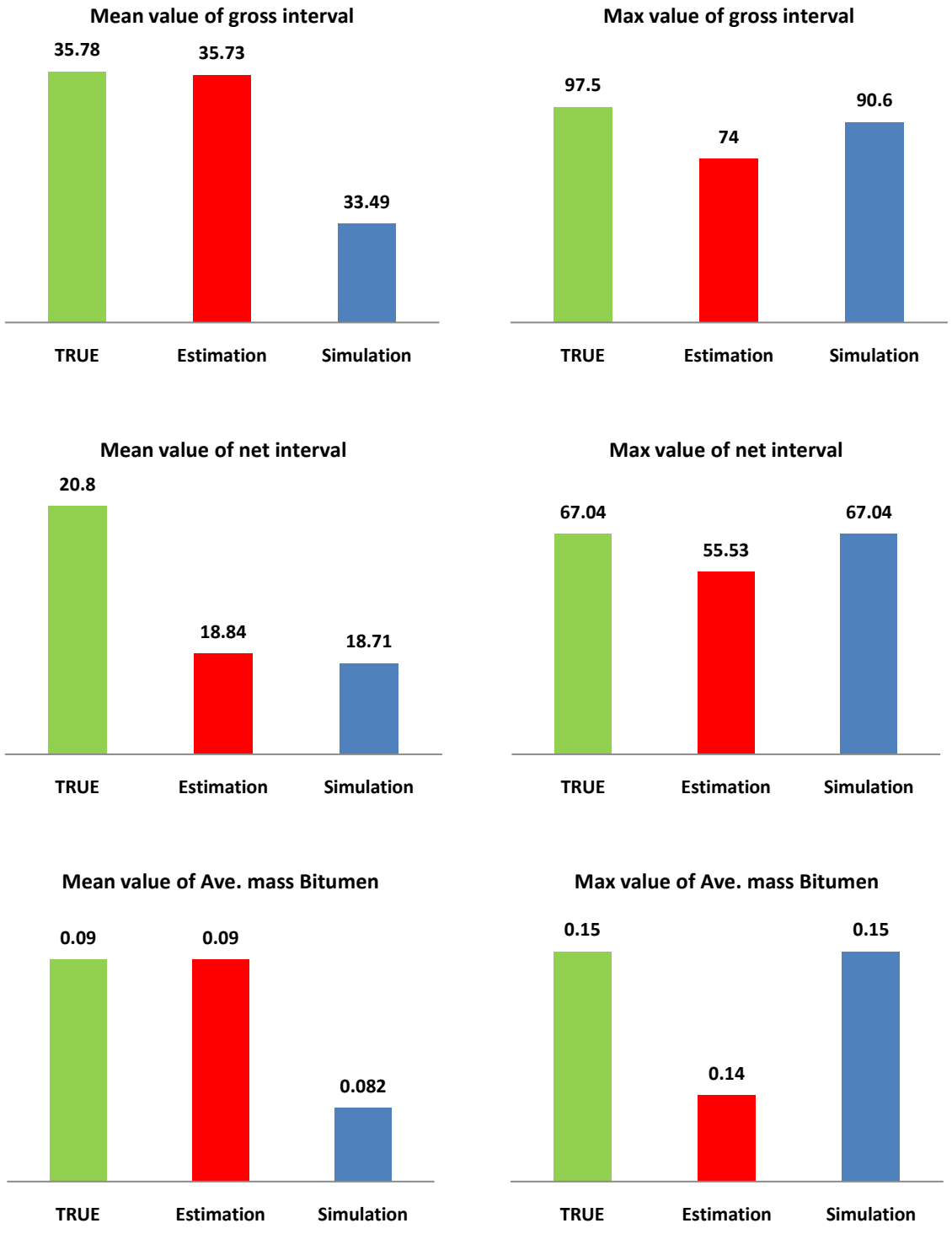

Fig. 44. Comparison of true values with the results from estimation and simulation

Table 17.of Bitumen in study area based on different methods

Method	Ave. Net interval (m)	Bbl of Bitumen $\times 10^9$	Bbl of Bitumen $\times 10^9$ (Based on fourth variable)	Difference from declustering (%)
Declustering	16.1	175	232	--------
Estimation	18.8	240	254	27
Simulation (avg)	18.7	204	260	14.2
Simulation (P10)	6.41	48	91	--------
Simulation (P90)	30.93	494	459	--------

4.7. Sensitivity analysis

To perform sensitivity analysis, the obtained results for mean uncertainty were used. For this purpose, the P_{10}, P_{50}, and P_{90} values of mean uncertainty were calculated for each variable using "quantile.exe" program. The results has been illustrate in Table 18. Afterwards, SK was done three times for each variable according to the obtained values for P_{10}, P_{50}, and $P_{90.}$ Average value of each variable after clipping has been represented in Table 19. It can be clearly seen that there is no significant difference between the results of SK with different means belong to uncertainty interval.

According to the presented value for P_{10} and P_{90} of net interval and Average mass Bitumen, amount of Bitumen for each of them was calculated. The result has been presented in Table 20. It can be seen that the amount of bitumen for estimation method and P10 and P90 values varies between 229 and 234 billion bbl.

Table 18.Obtained result from quantile program for P10, P50, and P90

	Spatial bootstrap of mean		P_{10}	P_{50}	P_{90}
	Min.	Max.			
Gross interval (m)	22.15	36.30	26.79	29.15	31.62
Net interval (m)	13.26	19.34	14.93	16.04	17.23
Ave. mass Bitumen (%Mass)	0.068	0.094	0.077	0.082	0.087

Table 19.Average of SK after clipping based on P10, P50, and P_{90} values belong to mean uncertainty interval.

	Average after cliping		
	P_{10}	P_{50}	P_{90}
Gross interval (m)	34.29	34.4	34.51
Net interval (m)	18.77	18.84	18.93
Ave. mass Bitumen (%Mass)	0.092	0.0931	0.0934

Table 20.Amount of Bitumen for estimation method according to the P_{10} and P_{90} values

	P_{10}	P_{90}
Net interval (m)	18.77	18.93
Ave. mass Bitumen (%Mass)	0.092	0.0934
Bbl of Bitumen ($\times 10^9$)	229	234

4.1. Conclusion

The predicting of porosity and permeability at unsampled locations of reservoir is one of the important problems in petroleum engineering. Micro modeling with core photograph data provides an improved understanding of porosity and permeability relationships within facies. The results of micro modeling show that in this case, the relationship between horizontal permeability, vertical permeability, and porosity are as shown in Eq. (7) to (9)

$$K_{H-effective} = 2973\ln(\phi) + 5712 \qquad (R^2 = 0.822) \tag{7}$$

$$K_V = 3099\ln(\phi) + 6653 \qquad (R^2 = 0.835) \tag{8}$$

$$K_V = 998\ln(K_{H-effective}) - 5111 \qquad (R^2 = 0.812) \tag{9}$$

For regional modeling four steps should be followed. These steps include (1) data assembly, (2) Preliminary statistics, (3) model building, and (4) post processing. In this paper reservoir of the McMurray was characterized using the regional modeling. Many different maps were created to reveal different aspects of the gross interval, net interval, average mass Bitumen and their uncertainty. P_{10} and P_{90} maps provide heterogeneity and uncertainty information on the gross interval, net interval and average mass bitumen.

As can be seen in Table 17, the calculated values are different. Some sources of errors which have caused these differences are mentioned below:

- Since wells are not distributed evenly, declustered averages are different from the original ones.

- It is not accurate to average net thickness and mass fraction of bitumen separately and multiply them in the rough estimation. Therefore, the rough estimate calculated using net and bit averages is not the same as the one calculated based on the fourth variable.
- The number of estimated points in Kriging where net thickness is larger than gross is not too high considering the total number of cells. Therefore, the average net thickness and the modified net thickness are almost the same (they are the same after rounding); but in simulation two variables vary more.
- The total estimated bitumen in place is almost the same for the two methods based on Kriging as opposed to simulation where the difference is significant.
- When simulation is applied it is more effective to use either net and bit variables or the bitnet in calculating reservoir estimates.
- P10 estimates show that at least there are 48 to 91 (using two different methods) billion barrels of oil in place by 90 percent chance.
- P90 estimates stand for 10 percent probable optimistic average which shows that there may be 459 to 494 (using two different methods) billion barrels of oil in place.
- Generally said, Kriging has resulted in higher estimate than simulation average which can be due to the smoothing effect of Kriging.

5. References

Deutsch, C. V. (2009). *Estimation of vertical permeabilty in the McMurray formation.* Paper presented at the Canadian International Petroleum Conference, Calgary, Alberta, Canada.

Deutsch, C.V. (2002). *Geostatistical Reservoir Modeling*. New York: Oxford University Press.

Deutsch, C.V. , & Journel, A. (1998). *GSLIB: geostatistical software library and user's guide* (2nd ed.): Oxford University Press.

Hein, F. J., & Cotterill, D. K. (2000). *An atlas of lithofacies of the McMurray formation, Athabasca oil sands deposit, Northeastern Alberta: surface and subsurface*: Alberta Energy and Utilities board.

Leuangthong, O., Khan, D., & Deutsch, C.V. (2008). *Solved Problems in Geostatistics*. New York: Wiley Inter science.

Ren, W., Mclennan, J.A., Leuangthong, O., & Deutsch, C.V. (2006). Reservoir Characterization of McMurray Formation by 2D Geostatistical Modeling. *Natural resource Research, 15*(2), 111-117.